CORA Cork Open Research Archive
Cartlann Taighde Oscailte Chorcaí

Title	New generation electron beam resists: a review
Authors	Gangnaik, Anushka S.;Georgiev, Yordan M.;Holmes, Justin D.
Publication date	2017-01-12
Original Citation	Gangnaik, A. S. Georgiev, Y. M. and Holmes, J. D. (2017) 'New generation electron beam resists: a review'. Chemistry of Materials, 29 (5):1898-1917. doi:10.1021/acs.chemmater.6b03483
Type of publication	Article (peer-reviewed)
Link to publisher's version	10.1021/acs.chemmater.6b03483
Rights	© 2017 American Chemical Society. This document is the Accepted Manuscript version of a Published Work that appeared in final form in Chemistry of Materials, copyright © American Chemical Society after peer review and technical editing by the publisher. To access the final edited and published work see http://pubs.acs.org/doi/abs/10.1021/acs.chemmater.6b03483
Download date	2026-11-08 16:10:20
Item downloaded from	https://hdl.handle.net/10468/3882

UCC
University College Cork, Ireland
Coláiste na hOllscoile Corcaigh

Subscriber access provided by UNIV COLL CORK

Review

New Generation Electron Beam Resists: A Review

Anushka S. Gangnaik, Yordan M. Georgiev, and Justin D. Holmes

Chem. Mater., **Just Accepted Manuscript** • DOI: 10.1021/acs.chemmater.6b03483 • Publication Date (Web): 12 Jan 2017

Downloaded from http://pubs.acs.org on January 20, 2017

Just Accepted

"Just Accepted" manuscripts have been peer-reviewed and accepted for publication. They are posted online prior to technical editing, formatting for publication and author proofing. The American Chemical Society provides "Just Accepted" as a free service to the research community to expedite the dissemination of scientific material as soon as possible after acceptance. "Just Accepted" manuscripts appear in full in PDF format accompanied by an HTML abstract. "Just Accepted" manuscripts have been fully peer reviewed, but should not be considered the official version of record. They are accessible to all readers and citable by the Digital Object Identifier (DOI®). "Just Accepted" is an optional service offered to authors. Therefore, the "Just Accepted" Web site may not include all articles that will be published in the journal. After a manuscript is technically edited and formatted, it will be removed from the "Just Accepted" Web site and published as an ASAP article. Note that technical editing may introduce minor changes to the manuscript text and/or graphics which could affect content, and all legal disclaimers and ethical guidelines that apply to the journal pertain. ACS cannot be held responsible for errors or consequences arising from the use of information contained in these "Just Accepted" manuscripts.

Chemistry of Materials is published by the American Chemical Society. 1155 Sixteenth Street N.W., Washington, DC 20036

Published by American Chemical Society. Copyright © American Chemical Society. However, no copyright claim is made to original U.S. Government works, or works produced by employees of any Commonwealth realm Crown government in the course of their duties.

New Generation Electron Beam Resists: A Review

Anushka S. Gangnaik, Yordan M. Georgiev†, Justin D. Holmes*

Materials Chemistry and Analysis Group, Department of Chemistry and Tyndall National Institute, University College Cork, Cork, Ireland and AMBER@CRANN, Trinity College Dublin, Dublin 2, Ireland

ABSTRACT: Semiconductor industry has already entered sub-10 nm region, which has led to the development of cutting-edge fabrication tools. However, there are other factors that hinder the best outcome of these tools, such as the substrate and resist materials, pre- and post-fabrication processes, etc. Amongst the most lithography techniques, electron beam lithography (EBL) is the prime choice when a job requires dimensions lower than 10-20 nm, since it can easily achieve such critical dimensions in reasonable time and effort. When obtaining pattern features in single nanometer regime, the resist material properties play an important role in determining the size. With this agenda in mind, many resists have been developed over the years suitable for attaining required resolution in lesser EBL writing time. This review article addresses the recent advancements made in EBL resists technology. It first describes the different lithography process briefly and then progresses on to parameters affecting the EBL fabrications processes. EBL resists are then bifurcated into their "family types" depending on their chemical composition. Each family describes one or two examples of the new resists; and their chemical formulation, contrast-sensitivity values and their highest resolution are described. The review finally gives an account of various alternate next-generation lithography techniques, promising dimensions in the nanometer range.

1 INTRODUCTION

Nanotechnology is the art and science of shaping matter in such a way that resulting structures (nanostructures) have at least one dimension between 1 and 100 nm. It covers a large range of scientific fields from chemistry, physics, biology and engineering to nanofabrication, surface science and medicine. Nanotechnology research is also very diverse and includes nanodevice fabrication, molecular self-assembly techniques and generation of new materials. Nanotechnology has enabled us to achieve advanced, superior and powerful products used for the betterment of human life.

One of the most prominent applications of nanotechnology is in the semiconductor industry, due to the miniaturisation of complex circuitry in microelectronic devices. This scaling down of size has pushed the scale limit of integrated circuits to beyond sub-50 nm and hence demands for fabrication methods with superior performance. There are two fundamental approaches on the basis of which nanofabrication is currently carried out: Bottom-up and Top-down approaches.[1] These two approaches can be applied individually or in combination. The top-down approach involves carving out nanostructures from bulk substrates and involves several processes, *e.g.* lithography combined with additive/subtractive processes of pattern transfer, such as thin film deposition, implantation, diffusion, etching, *etc*. Bottom-up approaches act in the reverse direction, *i.e.* the nanostructures are formed by starting from atomic/molecular elements, which are gradually assembled until the desired structure is obtained through processes such as self-assembly of molecules, nanoscaffolding, *etc*.

The top-down approach is still the prevailing technique in the micro- and nanoelectronics industry. Nanolithography plays a central role in this approach, where a stencil with the required pattern is created usually in a sacrificial layer called "resist", deposited on the main working material, like silicon (Si). There are various nanolithography techniques including deep ultraviolet (DUV) lithography, electron beam lithography (EBL), soft lithography, nanoimprint lithography (NIL), X-ray lithography, photon beam lithography (PBL) or scanning probe lithography.

1.1 THE PHOTOLITHOGRAPHY PROCESS

Photolithography is the most commonly used lithographic processes. It uses light of various wavelengths to create desired patterns. Typically, a suitable base substrate is coated with a thin film of a polymeric substance called a 'resist'. A photomask, usually made of ~80 nm thick patterned chromium metal layer deposited on a quartz plate, is held very closely or pressed against the resist-coated substrate and light of the desired wavelength is radiated on the mask for a certain time interval. The areas of the resist below the openings in the patterned chromium layer are exposed to the light and the irradiation brings about changes in the chemical structure of the underlying resist material. In most *positive*-acting resists, long polymer chains will break down into smaller components, whereas in *negative*-acting resists, polymer chains will crosslink on exposure to irradiation to form longer polymer chains. The substrate is then immersed in a specific solution called 'developer' and the exposed areas are selectively dissolved (positive) or remain insoluble (negative) in the solution. Subsequently, the substrate is ready for further processing, *e.g.* etching, metal deposition, *etc*.

Optical lithography is the most widely used patterning technique in the integrated circuit (IC) industry. During the past two decades, photolithography has matured and improved its capability to create very small features. However, with the ever-increasing demand for newer generation devices, the miniaturisation of device components has rapidly developed. Photolithography, due to its diffraction limits is unable to produce extremely small and densely populated features much below 50 nm. The diffraction effect from the mask openings and reflection effects within the resist, degenerate the quality of the obtained structures.[2] Deep ultraviolet (DUV) lithography has enabled to achieve resolution down to sub-50 nm, by employing wavelengths of 193 and 248 nm. Large-scale integrated ICs are currently fabricated by multiple exposures with immersion DUV lithography, but then again the equipment required is very expensive.[3] Techniques like extreme ultraviolet (EUV) and X-Ray lithography have also been developed, which use even shorter wavelengths than DUV, *i.e.* 13.5 and 10's nm (soft X-rays) down to 1 Å (deep X-rays), respectively. However, these approaches require complex and very expensive instrumentation.

1.2 THE CHARGED PARTICLES LITHOGRAPHY

In order to overcome the shortcomings of photolithography, alternative lithography techniques have been developed that uses charged particles instead of photons to create patterns. Using charged particles such as electrons, ions, or protons allows both patterning and imaging of a substrate. Whilst photolithography involves 'flood-type' exposure through a mask, direct writing can be achieved with a narrow beam of charged particles. This lithographic approach is a mask-less method, wherein desired designs are generated on computer software and then directly written with the particle beam onto a substrate. The beam sequentially writes the pattern, exposing point by point at a time or one pixel per interval. A small beam size, down to 1-2 nm, can be achieved by fine focusing and adjusting the aperture through which the beam passes. Due to the nature of charged particles, unlike photolithography, diffraction issue do not interfere with patterning thus yielding sub-20 nm size features very conveniently.

The most extensively used charged particle techniques are the electron beam lithography (EBL) and ion beam lithography (IBL). As the names suggest, the beam in the EBL consists of high-energy electrons that are used to write the desired pattern, whereas in IBL they are high-energy ions. Amongst the two, EBL, like photolithography, is a resist-based lithography. The EBL resists are specially formulated to undergo chemical reactions once they are exposed to high-energy electrons. IBL, on the other hand, may be used both with and without resist, since ions are much heavier than electrons and can easily mill substrates like silicon (Si) or germanium (Ge), carving the desired pattern. Both techniques are thus capable of producing very small structures, since the beams can be finely focused. However, exposure of patterns pixel by pixel increases writing time, especially for complex patterns with high design densities. Therefore, the throughput of EBL and IBL is low and hence these techniques are mainly used in research and development (R&D) as well as in small volume production and in industry for photomask fabrication.

In summary, although photolithography, in particular the DUV lithography, is still the main technique used for mass production in the semiconductor industry, beam lithographies and especially EBL is becoming increasingly widespread and is the dominant nanolithography method used in academic and research environments due to its flexibility and mask-less nature, very high (sub-10 nm) resolution as well as maturity and affordability of equipment.

2 PARAMETERS OF ELECTRON BEAM RESISTS

The techniques hitherto discussed, all have a common component without which they would be futile processes, namely a resist. Resists are usually polymeric materials that can be deposited on most surfaces that are subjected to patterning e.g. with photolithography or EBL. Many new commercial resists have emerged lately with the aim of improving resolution limits of lithography. In the following section, new EBL resists introduced over the last 5-6 years shall be discussed in detail.

Generally, a thin layer of the resist, ranging from 20-25 nm up to a micrometre is spin coated onto a substrate. The resist are usually organic or inorganic polymers and can be broadly classified into two types with respect to their tones, i.e. positive or negative. The electron beam irradiates the resist in such a manner that after development the radiated portion will be eliminated (*positive tone*) or will persist (*negative tone*) on the substrate. The patterning resolution of a polymer resist depends on its chemical structure. Achieving the best possible resolution with both positive and negative EBL resists requires manipulation of many parameters.

2.1 Contrast and Sensitivity

Contrast and sensitivity are the primary characterisation factors to be taken into consideration when choosing any resist. Contrast is the property of a resist to differentiate between exposed and unexposed areas. This is in turn coupled with a property known as sensitivity, which defines the extent of alteration in the resist material with respect to the electron beam dose. An electron dose is usually expressed in $\mu C/cm^2$ and is the number of electrons/electric charge per unit area required to achieve the desired changes in a resist.[4] Contrast and sensitivity together give rise to a contrast curve of a resist which is obtained by simply plotting the remaining resist thickness as a function of increasing electron beam dose. The plot shown in Figure 1 illustrates the contrast curves for a positive and negative resist. The plot shows the decrease (positive) or increase (negative) of the remaining resist thickness versus the exposure dose. According to the curve, the sensitivity is the dose D_{100} at which the resist is completely developed (for a positive resist) or reaches the full initial resist

thickness (for a negative resist) and contrast is the slope of the curve.

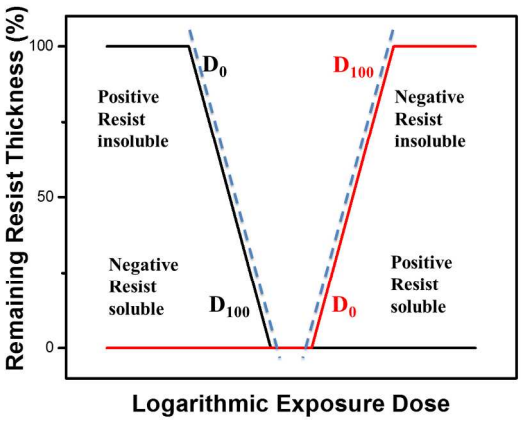


Figure 1. Typical contrast-sensitivity plots for positive and negative EBL resists

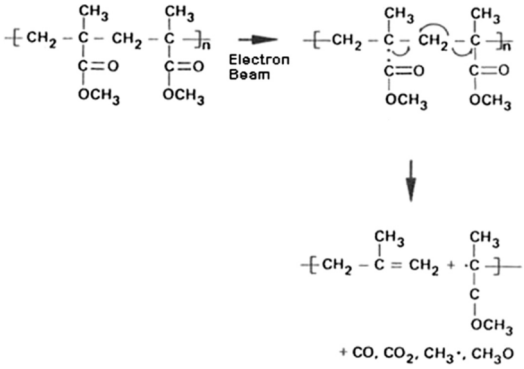
Sensitivity and contrast are expressed by the equation 1:[5]

$$\gamma = \frac{1}{\log \frac{D_{100}}{D_0}} \qquad (1)$$

where γ is the contrast value, D_o is the highest dose at which the resist is not yet affected by the electron irradiation (for a positive resist its thickness is still 100 % of the original thickness and for a negative resist its thickness is still 0), whereas D_{100} is the minimum dose at which the resist has undergone a complete change of its chemical structure.[6] Ideally, a resist must possess a high sensitivity and contrast. In reality however, an increase in one parameter will result in a decline of the other and vice versa. Hence, resists are often tuned to have a good balance of both parameters. Sensitivity of a resist varies with respect to resist type, electron energy, developer solvents and development conditions. Substrate materials to be patterned also play an important role.

2.2 Developer Solvents

Besides the resist properties, developer solvents, development time and temperature are among the most important factors that govern the contrast-sensitivity balance. Substrates, after the EBL exposure, are developed in solvents that separate the exposed from the unexposed resist. The resist-developer interdependency can immensely influence the contrast-sensitivity balance. Therefore, sensitivity and contrast are properties not only of the resist but rather of the certain couple resist-developer. For example, poly methylmethacrylate (PMMA) is the most well-established and extensively studied polymeric EBL resist. FTIR studies have shown that upon irradiation, PMMA chain-scission causes C=C bonds, which is soluble in the developer.[7] Scheme 1 illustrates the irradiation induced reactions in PMMA. Other methyl acrylate resists have also shown to follow similar chain-scission path.[8] Table 1 illustrates the effect on contrast, sensitivity and the surface roughness of PMMA resist having 950 K molecular weight (MW) by varying development conditions.



Scheme 1. Schematic representation of the mechanism of electron beam irradiation-induced reactions in PMMA films.[7]

Table 1. Comparison of sensitivity, contrast and surface roughness of PMMA (MW 950 K) for different development condition obtained with 19 kV beam.[6]

Developer	Sensitivity (μC/cm²)	Contrast γ	Max. RMS of surface roughness
IPA:MIBK 3:1 for 30 sec	100	4.3	4.2
IPA for 30 sec	250	6.1	5.9
IPA for 15 sec	270	7.2	4.4
IPA for 5 sec	300	7.6	3.1

Table 1 shows that isopropyl alcohol (IPA) and methyl isobutyl ketone (MIBK) in a 3:1 ratio, which is the standard developer for PMMA, exhibits a higher sensitivity than pure IPA for all time intervals. Conversely, the contrast is the highest for PMMA developed in a single component developer, IPA, for 5 s and is higher than IPA:MIBK by a

difference of 3.3. Moreover, surface roughness of the exposed area has also been reduced upon moving from IPA:MIBK to pure IPA. These factors impact on the lithographic performance of PMMA, as demonstrated in Figure 2.

Figure 2(a) shows that the 50 nm gratings achieved by an electron dose of 180 μC/cm² at 19 keV exhibit poorly defined structures when developed with IPA:MIBK. With pure IPA, however, the 50 nm gratings are very well resolved although the sensitivity is reduced to 750 μC/cm². Reduced sensitivity but improved contrast is therefore achieved using IPA as a developer, as opposed to IPA:MIBK, for EBL lithography of PMMA resist.

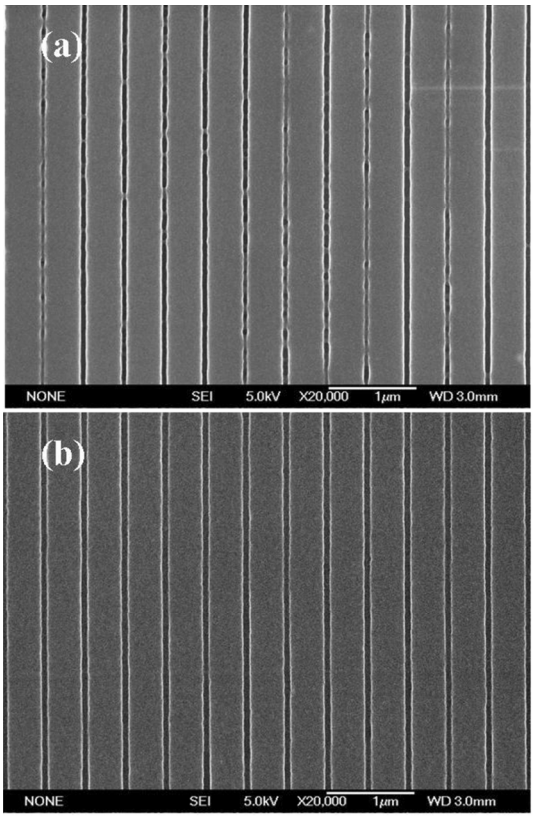


Figure 2. Scanning electron microscopy (SEM) images of semi-dense line arrays in PMMA resist with a 50 nm linewidth. The arrays are exposed with dose of (a) 180 μC/cm² and (b) 750 μC/cm² and developed with (a) a IPA:MIBK *3:1* mixture for 30 s and (b) IPA for 5 s.[6]

2.3 Temperature

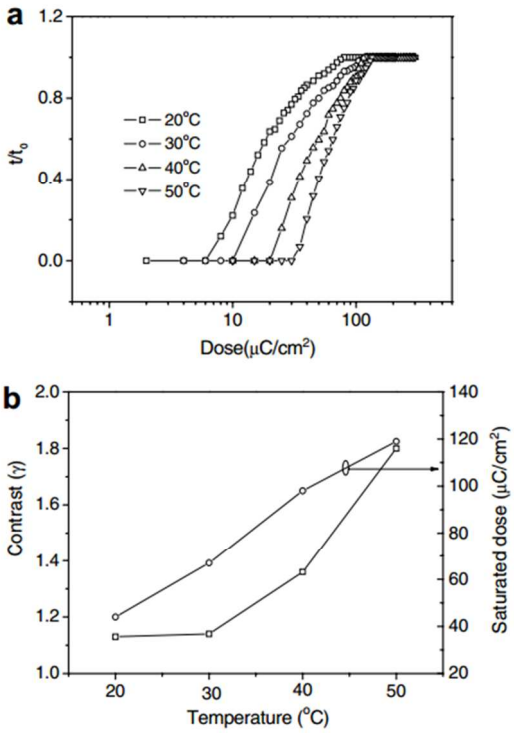


Figure 3. Development temperature dependence of (a) contrast curves for HSQ resist (100 kV) and (b) variation of the contrast and saturation dose with the development temperature in 2.5 % TMAH developer.[9]

The temperature of a developer can also affect the lithographic performance of a resist. Hydrogen silsesquioxane (HSQ) is a negative tone EBL resist having very high (sub-5 nm) resolution, high etch resistance and is very stable during scanning electron microscopy (SEM) inspection. In a study on the temperature dependence of development results, contrast curves for HSQ were obtained at different temperatures in a 2.5 % TMAH (tetramethylammonium hydroxide) developer. The temperatures were varied from 20 to 50 °C and the results are presented in Figure 3.[9]

Figure 3 shows that the temperature of the developer has a considerable effect on the contrast-sensitivity of HSQ resist. As the temperature is raised from room temperature (20° C) to 50° C, the contrast is improved but at the cost of reduced sensitivity. The main reason for this is that warm developers are more effective in dissolving the resist molecules than the cold ones. Therefore, at room temperature the developer is not able to dissolve the resist areas that are partially exposed by forward- and backscattered electrons (only partially cross-

linked), leading to good sensitivity (less primary dose necessary to form a resist structure remaining on the substrate) but poor contrast. At elevated temperatures, however, the partially exposed resist is completely dissolved, which results in lower sensitivity (more primary dose necessary to form a resist structure remaining on the substrate) but higher contrast (better differentiation between exposed and unexposed or partially exposed resist).

In the case of a positive resist, the opposite effect is observed, *i.e.* cooler developer solutions have shown to improve the contrast immensely, however negatively affecting the sensitivity.[11] Here the reason for this behaviour is again the same as with the negative resists but working in the opposite direction, since the electron exposure dissociates the molecular bonds in positive resists, causing scission of molecules, whereas it cross-links the molecular bonds in negative resists, causing networking of molecules. Therefore, at room temperature the developer is able to dissolve the partially exposed positive resist, leading to good sensitivity (less primary dose necessary to remove the resist from the substrate) but poor contrast. At low temperatures, however, the partially exposed positive resist is not dissolved by the developer, which results in lower sensitivity but higher contrast. Figure 4 illustrates the contrast curves of the positive resist SML at different voltages developed in a 7:3 ratio of IPA:water.[10] Two developer temperatures were employed, *i.e.* room temperature and 0 °C. The plot shows that the sensitivity of the resist developed at 0 °C is reduced by 4 times compared to room temperature and the contrast is moderately increased (by approximately 1.6 times).

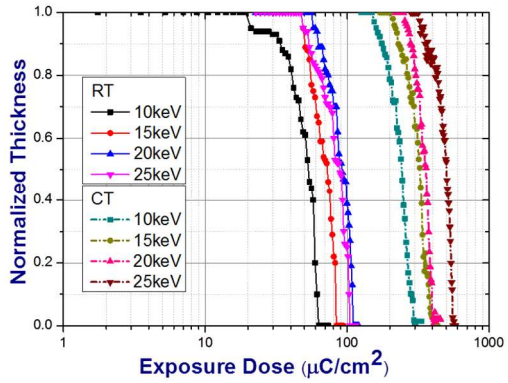


Figure 4. Contrast curves of SML 50 developed in a 7:3 ratio of IPA:water developer at cold temperature (0 °C) and at room temperature.[10]

2.4 Auxiliary Factors

In this section supplementary important factors that contribute to resist profiling are briefly discussed. Technical restrictions arising from a particular lithography tool also contribute to the resolution of the resist. EBL systems are usually designed with voltages from 1 to 30 keV, for converted SEMs, and from 25 to 100 keV for dedicated systems. The sensitivity and resolution of a resist depends largely on the energy of the electron beam. For any resist, the sensitivity decreases when higher voltages are employed whereas the contrast (resolution) improves. The main reason for this is that slow electrons interact more readily with solids and hence they expose the resist much more efficiently than fast electrons. Therefore, resists are more sensitive to irradiation with low-energy electrons than with high-energy electrons. This is clearly seen in the Bethe equation, which describes the mean energy loss per distance of fast non-relativistic electrons in solids:

$$-\frac{dE}{dx} = \left(\frac{2\pi e^4 \rho_{eff} Z_{eff}}{E A_{eff}}\right) \ln\left(\frac{1.166E}{J_{eff}}\right), \qquad (2)$$

where e is the electric charge of an electron, E is the electron energy, ρ_{eff}, Z_{eff}, A_{eff}, and J_{eff} are the effective mass density, atomic number, atomic weight, and mean ionisation potential of the target, respectively. Since the energy loss of the electrons is approximately proportional to E^{-1}, the higher the initial energy of the electrons, the less efficient is the energy deposition in the resist.

Another important fact is that the electrons are light particles and they are easily scattered in solids. Therefore, when a resist is exposed to an electron beam, it is irradiated by the primary electrons on their first passage through the resist (forward scattered electrons) as well as by electrons that have already reached the substrate and are scattered back into the resist (backscattered electrons).[11] In addition, secondary electrons generated by both forward and backscattered electrons also irradiate the resist. These phenomena leads to the fact that the resist is exposed not only in the intended areas but also in wide adjacent regions, causing a distortion of the designed pattern known as a "proximity effect".[12] At low energies, *e.g.* 10 keV or less, forward scattering is high, causing significant widening of the electron beam. In addition, backscattered electrons have a short range and are confined around the point of incidence of the electron beam causing substantial exposure of the resist. Therefore, at low electron energies the

proximity effect is relatively high and may lead to considerable distortion of the exposed pattern. Conversely, at high electron energies, *e.g.* 100 kV, the proximity effect is relatively less pronounced and the exposed pattern is usually closer to the original design.

Thus, for low resolution and large structures, *i.e.* micron sizes and above, low energy beams can be used to reduce the exposure time. For critical high-resolution patterns, however, high energies are needed. For instance, Figure 5 illustrates a germanium-on-insulator (GeOI) test device structure designed and patterned to measure the resistance across a nanowire having a width of 20 nm. This device was fabricated at two different exposures: the nanowires were fabricated at 10 keV with a fine electron beam whereas the contact pads were exposed at 1 keV with a large electron beam. At 10 keV the writing time for the large contact pads would have been approximately 15 minutes, however due to the lower voltage and the larger beam used the writing time was reduced to 1 minute.

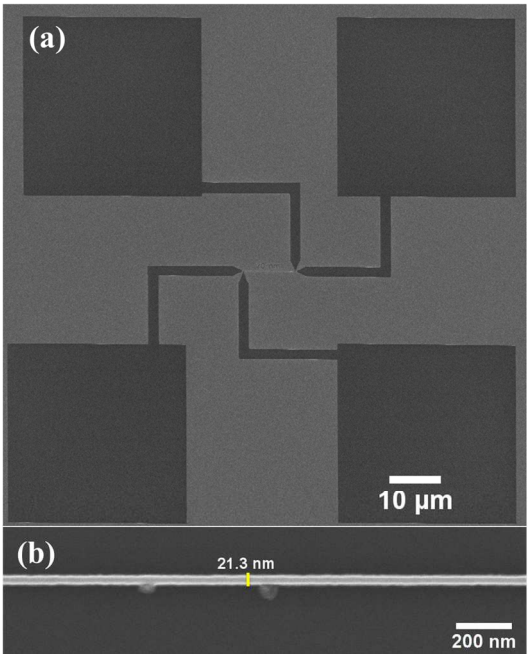


Figure 5. SEM micrograph of a test device on germanium on insulator for measuring the resistance across a 20 nm wide nanowire. (a) Low-resolution contact pads and contacts are exposed with 1 kV beam; (b) high-resolution 20 nm nanowire exposed with a 10 kV beam.[13]

Roughness of resists is another crucial resist parameter. As the critical dimensions go into the lower tens of nanometre, the line edge roughness (LER) and line width roughness (LWR) become crucial for the overall lithographic performance. Resist roughness is influenced by various factors like molecular weight of the polymer, the phase separation and polymer aggregation it undergoes in a developer solvent and irradiation dose. A bell-shaped curve of the root mean square roughness versus electron beam dose has been observed for positive resists and has been explained as a result of different rate of phase separation occurring at various doses .[14,8] Figure 6 is an example of the bell-shaped roughness curve of PMMA resist developed in 1:4 MIBK:IPA. The roughness can, however, be controlled by appropriate choice of developer solvent for a resist.

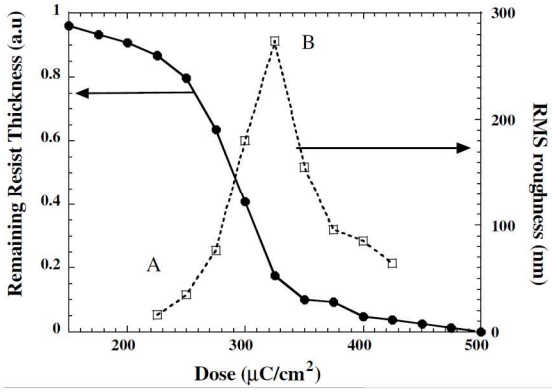


Figure 6. Experimental contrast curve and corresponding RMS roughness, for 2300 k PMMA resist using dip development at 25 °C for 30 s with 1:4 MIBK:IPA exposed with 50 kV beam.[14]

Similar dependence of the root mean square roughness versus electron beam dose has been observed also for negative resists.[15,16] Georgiev et al. have found that HSQ roughness depends on the developer concentration (in this case tetramethylammonium hydroxide, TMAH) and especially on the pre-exposure bake temperature. It has been shown that a combination of a strong developer with low baking temperature delivers low HSQ roughness and is favourable for achieving high resolution with this resist. Moreover, drying processes after resist development and rinsing can also have a significant impact on resist roughness. For example, supercritical CO_2 drying has been shown to significantly reduce HSQ roughness and improve stability of high aspect ratio lithographic structures. [17]

International technology roadmaps for semiconductors (ITRS) stated that the LER and LWR should be less than 8% of the critical dimension, since they can directly influence the device performance.[18] With the aggressively reduced critical dimension in the current and future

semiconductor technology nodes, this requirement is a significant challenge to resist performance. Roughness is thus becoming an important leg in nanolithography.

3 EBL RESIST FAMILIES

EBL is a direct-write process and due to the lightweight nature of the electrons, the beam cannot engrave typically used substrate materials. Resists are thus an integral part of an EBL process. The resist pattern produces a stencil on the substrate, which can be transferred into the substrate with further fabrication processes. Over the years, many new resists have been formulated to fulfil various micro- and nanofabrication demands. Traditional resists like PMMA, ZEP and HSQ are the most commonly used ones due to their superior lithographic outputs. This section will highlight new classes of EBL resists that have been introduced during the past 5-6 years.

While defining electron resists, the aforementioned words PMMA, ZEP and HSQ appear regularly in the literature. Most of the literature reports on resists, irrespective of resist tones, often consider these resists as standard for resolution comparison with new resists.[4,9,10,19] HSQ (Dow Corning) is the commercially available resist that has provided the highest resolution EBL structures down to sub-5 nm.[20] HSQ is an inorganic material belonging to the spherosiloxane family, with a low dielectric constant (2.8).[21] HSQ's high-resolution capability, ease of imaging post-exposure and etch resistance are its prominent features. However, the resist suffers from several drawbacks, such as a very limited shelf life of up to 6 months and a necessity to be stored at a temperature below 5 °C, thus requiring a high standard of maintenance. HSQ is extremely sensitive to moisture and hence the interval between spin casting and exposure must be as minimal as possible to avoid unsolicited crosslinking of polymer molecules. From the lithography point of view, the resist suffers a relatively low sensitivity, *e.g.* an electron dose of between 900-1000 $\mu C/cm^2$ is required to generate a 50 nm wide line on Si at 10 kV, which eventually increases the writing time in comparison with PMMA (~330 $\mu C/cm^2$) and especially ZEP (~120 $\mu C/cm^2$). Thus, even though HSQ exhibits commendable lithographic qualities, it is still a difficult resist to handle.

PMMA is a well-established positive resist having a good balance of sensitivity, contrast and roughness. Therefore, it is by far the most widely utilised EBL resist. PMMA with different molecular weights can be used in various applications involving EBL fabrication. Sub-10 nm resolution structures have been demonstrated with PMMA using high beam voltages and cold temperature developments, thus requiring higher electron beam doses.[22] The positive resist ZEP was developed around the end of 1980's.[23] Early studies showed its commendable resolution, better etch durability and sensitivity improvement (one order of magnitude) in comparison to PMMA.[24] However, over the last couple of years the commercial value of ZEP has risen by tenfold in Europe making it tremendously more expensive than PMMA.[25]

Many new resists have emerged in the past few years. Other than their lithographic perspectives, aspects such as cost, shelf life, perilousness and compatibility with industrial semiconductor processes need to be taken into account. Resists are broadly classified into two divisions, positive and negative, depending on their reaction upon e-beam radiation. However, based on their chemical structures, they can be further classified into families, irrespective of their tones.

3.1 Chemically Amplified Resists (CARS)

A family of resists known as chemically amplified resists (CARS) emerged in the 1980's as powerful lithographic materials due to their supreme sensitivity and resolution.[26,27] These resists were initially proposed and developed by IBM as photoresists but are now also regularly used for EBL.[27] They are basically a blend of an acid reactive polymer, such as an epoxy group based polymer, and a photo-acid generator (PAG).[28,29] They are also formulated in the two tones of the resists. Upon electron irradiation, the photo-acid is released which catalyses further reactions without an additional electron dose, thus enhancing sensitivity. The substrate is then baked after exposure in order for the released photo-acid to catalyse the resist matrix.[4] However, as device miniaturisation has continued, several factors have affected the resolution of CARS. Firstly, the non-uniform acid diffusion and migration within the resist film during post-exposure baking limits the critical resolution of CARS.[30,31] Secondly, as a result of acid diffusion, roughness in patterned structures arises. Thus, controlling acid diffusion is a priority to acquire high-resolution feature sizes from CARS. One of the methods used to overcome this problem was to bond a PAG unit to the polymer sidechain, rather than blending the PAG with the polymer.[31] Thus,

several polymer-bound PAG CARS have been developed over the last few years.

Polymer-bound PAG resists are therefore usually a merger of complex polymers. Recently, such a negative tone CAR comprising of glycidyl methacrylate (GMA), methyl methacrylate (MMA) and triphenlysulfonium salts methacrylate (TPSMA) was developed for EBL and was compared with a polymer blended PAG CARS for sensitivity and contrast.[32] Firstly, the two polymers were polymerised together to give the product poly (GMA-co-MMA) which was further polymerised with the PAG to give poly (GMA-co-MMA-co-TPSMA) powder (Avg. Mol. wt. = 23,800 g/mol). The resist solution was prepared by dissolving the powder in dimethylformamide (DMF) or propylene glycol monomethyl ether acetate (PGMEA). Their sensitivity, lithographic performance and etch resistance were evaluated in the study. The contrast curve of the first CAR revealed a sensitivity of 300 μC/cm² without any post-exposure bake. The sensitivity of the second polymer mixture, poly (GMA-co-MMA-co-TPSMA), was measured as 125 μC/cm² with a 100 kV beam without post-exposure bake, which further reduced to 70 μC/cm² by post-exposure baking at 80 °C for 60 s. The resists were developed in a mild 7:3 ratio of IPA:water developer solution for 1 min followed by rinsing in deionised (DI) water. The smallest feature size that was acquired from the resist was a 15 nm line with a 1:15 pitch size, as illustrated in Figure 7(a). Dense grating of 20 nm lines using a 1:1 pitch size was also obtained and shown in Figure 7(b). However, post-exposure bake accelerated acid diffusion in the resist, thus unfavourably affecting the line edge roughness (LER), as shown in Figure 7 (c). The post-exposure bake can however be excluded, hence cutting down a process step at the expense of lower sensitivity. The RIE etch rate of the resist was determined to be 40 nm/min with CF_4 gas chemistry.

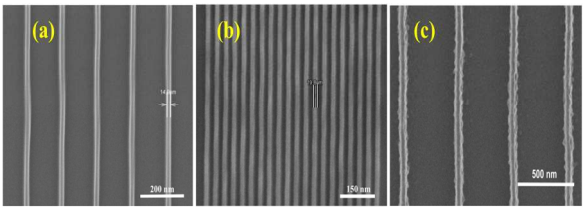


Figure 7. SEM images of gratings produced using the negative tone poly (GMA-co-MMA-co-TPSMA) resist: (a) 14 nm grating with a 1:15 pitch, (b) dense gratings with a 19 nm linewidth in 1:1 pitch and (c) gratings with post-exposure bake at 80 °C for 60 s.[32]

Positive tone CARS have also been employed and one of them recently used for EBL is 40TX. Such resists, when employed alone, produced an almost insoluble top layer due to the reaction between photo-acid evaporation and vapour contaminants.[33,34] Therefore, in a study a protective coat was spun on the CA resist which was comprised of acidic poly (3,4-ethylenedioxythiophene) poly(styrene-sulfonate) (PEDOT:PSS).[35] Contrast curves were generated for the resist at 20 keV using the standard developer AZ® 726MIF in various dilutions with DI water. The high sensitivity range of this resist lies between 7-10 μC/cm² and the contrast varies from 7-14. The effects of various developer dilutions on contrast-sensitivity values are given in Table 2. The critical dimension (CD) of the resist in this study was measured after a complete lift-off process, hence the CD values were between 80 to 110 nm as shown in Table 1.2. Gold nano-gratings, approximately 90 nm in width and 70 nm apart, were fabricated using this resist, as illustrated in the SEM image shown in Figure 8. The purpose of the study was to fabricate robust structures with this CAR, as there were no significant linewidth or sensitivity variations observed even when the samples were stored for 24 h in vacuum or air.[35]

Table 2. Contrast and sensitivity values of 40XT positive CARS for different development parameters.[35]

Developer Dilution (% vol. DI water)	Development time (s)	Contrast(γ)	Sensitivity (μC/cm²)	Critical Dimensions (nm)
0%	5	8 ± 2	8	95 ± 10
0%	10	7 ± 0.5	7	110 ± 5
33%	20	14 ± 2	10.5	No undercut
33%	40	10 ± 0.5	9	85 ± 5
33%	60	9 ± 0.5	8	85 ± 5
40%	60	11 ± 0.3	9	80 ± 5
40%	120	10 ± 0.3	7.5	80 ± 5

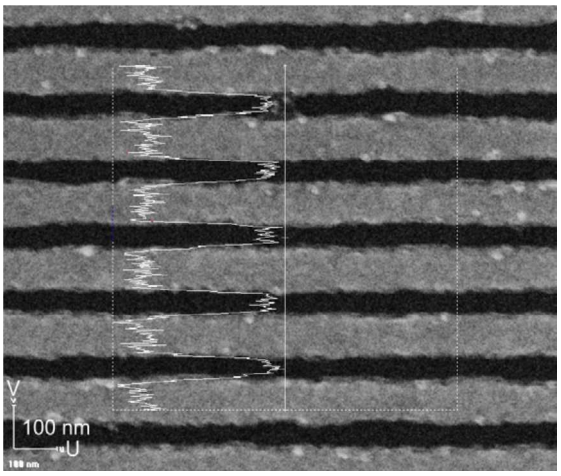


Figure 8. Line and space pattern: 90 nm wide gold lines on a SiO2 substrate spaced 70 nm apart (80 nm half-pitch), structured with the after lift-off process with 40XT/PEDOT-PSS. The sample was developed for 60 s in a developer diluted with 40 % vol. DI water.[35]

3.2 Non-CARS

Whilst CARS have demonstrated extremely high sensitivity, the LER and line width roughness (LWR) constrain the achievement of sub-20 nm feature size with them, as acid diffusion in the resist is uncontrolled at this scale.[36] To counter this effect, advanced classes of resists are being formulated which are directly sensitive to radiation and do not contain a PAG moeity.[37] In order to increase the irradiation sensitivity, a radiation sensitive group must be incorporated into the polymer unit. Such resists are known as non-chemically amplified resists (n-CARS). Sulphonium salts have been known to be sensitive to UV and electron beam radiations and can be incorporated into polymer units.[38] In a recent study, a copolymer of (4-(methacryloyloxy) phenyl) dimethylsulfonium triflate (MAPDST), the radiation sensitive group, and methyl methacrylate (MMA) was synthesised (MAPDST–MMA).[39] This copolymer was dissolved in methanol to give a negative tone resist solution. The copolymer resist coated substrates were exposed to electrons at 20 kV and were subjected to post-exposure bake at 100 °C for 120 s, followed by development in a 0.022 N TMAH solution. The customary characteristics of this resist were evaluated. The exceptionally high sensitivity of 2.06 μC/cm² was observed with a contrast of 1.8, which can be seen in the contrast curves shown in Figures 9(a). In Figure 9(b), the highest resolution lines of 20 nm width, with 100 nm spacing, are illustrated. These lines were obtained at a dose as low as 40 μC/cm², in contrast to the popular negative HSQ resist, which requires a dose close to 2000 μC/cm² to pattern lines of similar width and spacing. The gratings also exhibited a reasonable LER of between 1.8 to 2.2 nm.

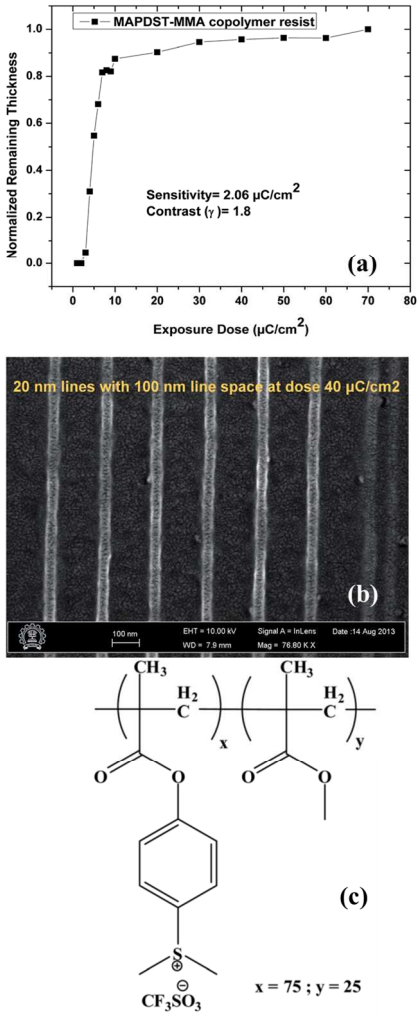


Figure 9. (a) Contrast curve of MAPDST-MMA copolymer negative resist, (b) SEM image of the electron beam patterning of the negative tone copolymer resist for isolated 20 nm line patterns with 100 nm space; patterns exposed at a dose of 40 μC/cm2.[39]

It was demonstrated by FTIR and XPS characterisation that irradiation of the resist strongly reduces triflate and COO group signals, whereas the S-C bonding belonging to the phenyl group remains resistant to the exposure.[40] Since the unexposed resist remains polar because of its ionic character (Figure 9 (c)), it can readily solubilise in the developer. On the other hand, upon irradiation

the anionic counter ions ($CFSO_3^-$) result in the formation of Ar-S^+-$(CH_3)_2$ groups, which convert to Ar-S-CH3 during the post-bake, losing thier ionic character.[41] Due to its non-ionic nature, the exposed resist was intact when dipped in developer solution. Hence, the addition of a highly radiation-sensitive sulphonium group to the polymer unit enhances the sensitivity of the resist tremendously. Structures as fine as 20 nm could be easily resolved with this resist. LER was found to be 1.8±0.1nm of MAPDST-MMA resist.[41] Thus, this resist is a good candidate for future high resolution EBL due to its high sensitivity and contrast and ability to generate low LER structures. The etch ratio of the MAPDST-copolymer to SiO2 with CHF_3/O_2 gases (22.5/2/5 sccm, 80 mTorr, 150 W RF power for 60 s) was found to be 0.36:1.[39]

However, in another study, a methacrylate based n-CARS was formulated that exhibited a very high sensitivity. The resist was created by free radical polymerisation of 2-hydroxyethyl methacrylate (HEMA) and aminoethyl methacrylate (AEM) to give the product poly(2-hydroxyethyl methacrylate-co-2-methacrylamido-ethyl methacrylate) (P(HEMA-co-MAAEMA)).[42] Its processing parameters and etch durability as a mask on Si were assessed. The contrast curves of the resist showed an extremely high sensitivity of about 0.89 $\mu C/cm^2$ and a contrast of 1.2 (figure 10(a)), which is comparable to the commercially available low-contrast negative EBL resists such as mr-EBL 6000 and AR-N 7720. The contrast curve was obtained by developing a 1.1 μm thick film in methanol developer. However, as shown in the AFM image and its corresponding cross-section in figure 10(b), the resist demonstrates a low resolution up to 125 nm. The authors, nevertheless, suggest that the resolution can be improved by modifying the development process, using thinner resist films or by modifying the accelerating voltages. Etch resistance of this resist was studied for RIE (SF_6), as well as, for wet chemistry with in HNA (HF: nitric acid: acetic acid) solution. The resist showed good resistance to the wet etch process and where the resist to silicon selectivity was 1:9.4 (etch rate of resist was ~15-20 nm/min). However, the resist performed poorly when subjected to dry etch since the resist to silicon etch rate ratio was found to be 1:2 and the etch rate of the resist was 225-275 nm/min.

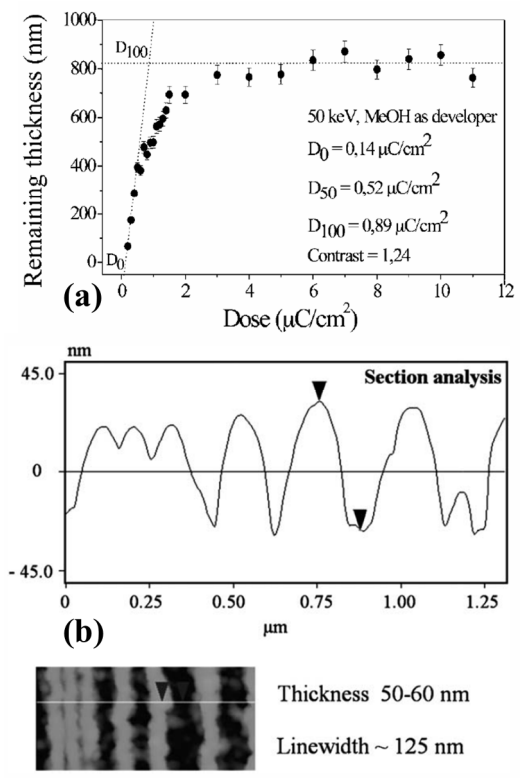


Figure 10. (a) Contrast curves of P(HEMA-co-MAAEMA) resist exposed at 50 kV and developed in methanol; (b) AFM image of exposed P(HEMA-co-MAAEMA) lines at a dose of 300 pC/cm. The pitch ranges from 100 to 300 nm from the left to the right. The corresponding cross-section is shown above the AFM image. The resist thickness is 50–60 nm, and linewidth ~125 nm.[42]

3.3 Fullerene Derivatives Resists

Buckminsterfullerene (hence after referred as fullerene), C_{60}, is an allotrope of carbon containing 60 C-atoms to form a spherically shaped unit. Fullerene's potential as a negative tone EBL resist was first recognised by Tada et al. due to its reactivity towards UV light.[43] C_{60} has small diameter, of around 0.7 nm, making it ideal for high-resolution lithography.[44] Tada et al. showed that electron beam irradiation caused the solubility of a C_{60} film to reduce in a toluene developer, thus allowing it to be used as a negative-tone resist.[43] However, C_{60} has a very low sensitivity of about 12 mC/cm^2 and requires preparation via vacuum sublimation.[45] Nevertheless, in the last few years, new types of polymer-bound fullerene derivative resists have been synthesized, which can be spin coated onto substrates. Two such resists, C_{60}-containing poly (p-tert-butoxystyrene) and C_{60}-

containing poly (p-tert-butoxycarbonyloxystyrene), have been developed for photolithography.[46] In the case of EBL resists, two of the fullerene derivatives developed in recent years, with different polymer chains, shall be discussed in the section below.

The first study involved the blending of two polymers, poly (*p*-chloromethlysytrene) (PCMS) and poly (hydrostyrene) (PHS), in which the C_{60} moiety was incorporated.[47] The main motivation behind using the PCMS polymer was its high electron sensitivity, whereas C_{60} alone has a tremendously low sensitivity of approximately 10^4 μC/cm^2.[43,48] The PHS was used because the hydroxyl group aids in the adhesion of the C_{60} derivative resist to a substrate. Various blends of the three unities consisting of different weight fraction of C_{60} have been produced, as shown in Table 3.

Table 3. Blends of PCMS and PHS polymers consisting of different weight fraction of C_{60} for preparing the resists.[47]

Code	Yeild (%)	M_n Calculated	Wt. fraction of C_{60} (wt%)	T_g (°C)
C_{60}-$(PCMS)_2$			7.6	90
C_{60}-$(P(CMS^{46}$-HS))$_2$	89	7700	9.4	>130
C_{60}-$(P(CMS^{31}$-HS))$_2$	96	7500	9.6	>130
C_{60}-$(P(CMS^{14}$-HS))$_2$	95	7900	9.1	>130
C_{60}-$(PHS)_2$	94	5400	13	>130

The resist-coated substrates were exposed to electrons at 100 kV and developed with toluene or acetone to evaluate their lithographic performance. Figure 11 illustrates the reaction mechanism of a C_{60} derivative resist upon electron beam radiation. The C60 derivative shown in Figure 10 is coded as C_{60}–(P(CMSx–HS))2 where x = 14, 31 or 46, thus varying the weight fraction of C60, according to Table 3. The developer used was acetone however strong aggregations of C_{60} moieties were found, which resulted into swelling and deformation of the structures. Figure 12 shows an SEM image of 50 nm gratings, the minimum resolution obtained with C_{60}-(P(CMS14-HS))2, at a dose of 286 μC/cm2 and a LER of ~7 nm.

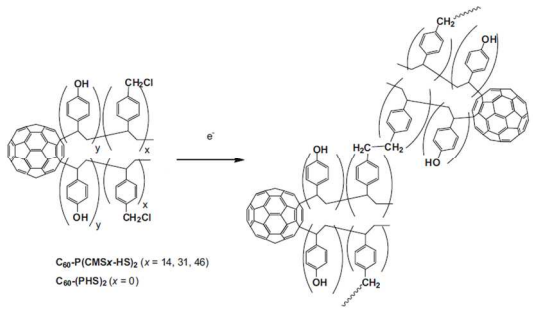


Figure 11. Crosslinking of the C_{60} derivative upon electron beam radiation.[47]

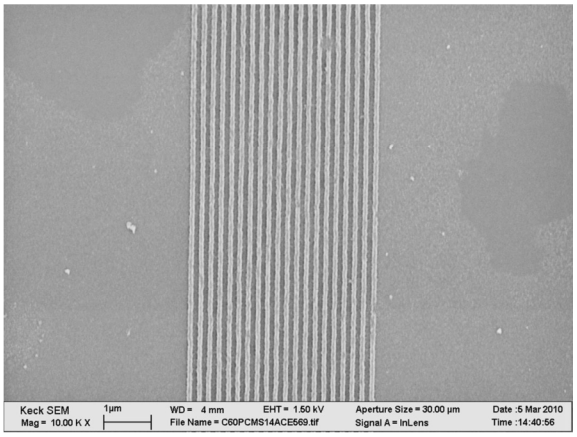


Figure 12. SEM image obtained after EB exposure using C_{60}-(P(CMS14-HS))2, at a dose of 286μC/cm2 and developed in acetone for 10 s.[47]

The C_{60}-$(P(CMS_{14}$-HS))$_2$ resist gave the best result in terms of resolutions amongst the other compositions given in Table 3. Hence, it was concluded that C_{60}-could be utilised as negative tone EBL resists. The sensitivity of the C_{60} moiety was increased by 3 orders of magnitude with the addition of the copolymers, achieving high-resolution structures down to 50 nm in each case.

In the second recent study, three phenol-based fullerene negative tone resists have been presented for next generation electron beam lithography.[49] The resist was not only a fullerene derivate, but also a CAR consisting of a crosslinker and a PAG component. The first fullerene derivative prepared consisted of phenolic methanofullerene (IM-MFP12-3). The other two resists consisted of tertiary butoxycarbonly (tBOC) protecting groups, however they differed in that one had a longer side chain (IM-MFP12-8) than the other (IM-MFP12-2). The resists were prepared by dissolving the fullerene derivative, epoxy crosslinker and

triphenylsulphonium hexafluroantimonate PAG in propylene glycol monomethyl ether (PGME), with a 10-20 g/L concentration. They were then mixed in one part fullerene derivative, two parts crosslinker and one part of the PAG and spin-coated onto Si substrates. The chemical structure of the three fullerene derivatives along with their contrast curves can be seen in Figure 13.

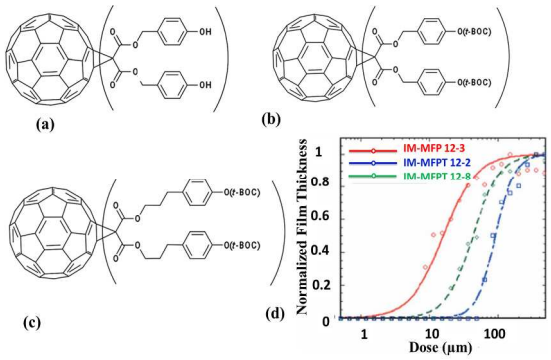


Figure 13. Chemical structures of (a) (3-phenol-1-propyl malonate)-methano-[60] fullerene, (b) (t-butoxycarbonyl malonate)-methano-[60] fullerene and (c) [3-(4 butoxycarbonyl) phenyl-1-propyl malonate]-methano-[60] fullerene and (d) contrast curves for the three resist derivatives.[49]

The Si substrates were post-exposure baked at 90 °C followed by dip development in 1:1 monochlorobenzene (MBC) and IPA. Figure 13(d) shows the calculated contrast curves of the three resists and their sensitivity (contrast in brackets): 93 μC/cm² (1.8), 43 μC/cm² (1.3) and 32μC/cm² (1.0) for IM-MFP12-2, 3 IM-MFP12-8 and IM-MFP12-3, respectively. Thus the enhanced sensitivity, amongst the tBOC-protected material, of IM-MFP12-8 was attributed to the higher flexibility of longer polymer chains helping to improve crosslinking. Long chains have previously been reported to enhance acid diffusion, which is evident in this study.[50]

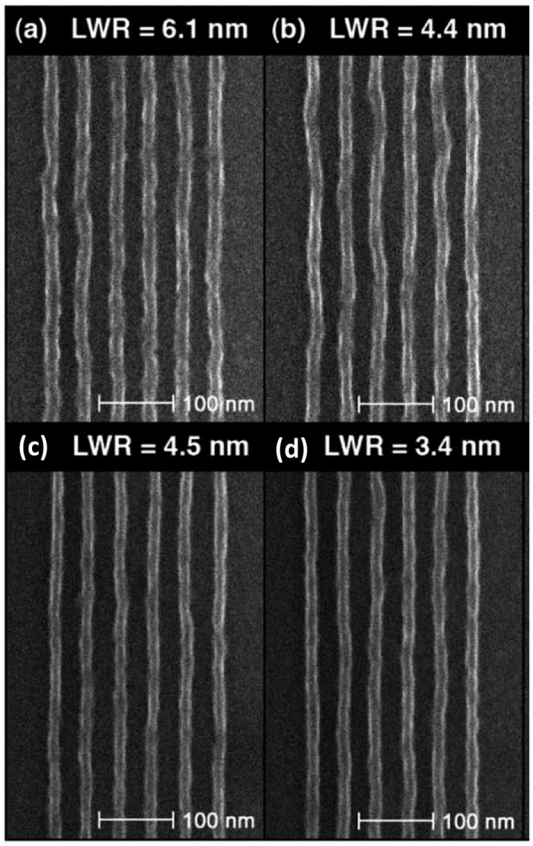


Figure 14. SEM images of dense single pixel features of IM-MFP12-8 resist, with the top row developed without post-exposure bake and the bottom row with 90 °C post-exposure bake. The pitches are 48 nm for (a) and (c); and 46 nm for (b) and (d) with their corresponding LWR.[49]

Figure 14 illustrates the SEM images of single pixel gratings exposed on IM-MFP12-8 resist developed with 1:1 MBC:IPA. The linewidth observed for the gratings lies between 13-15 nm; exposed at 30 kV within a dose range of between 240-350 pC/cm². From the SEM images shown in Figure 14, LWR is higher for exposures developed without the post-exposure bake, thus indicating the requirement of post-exposure bake for the complete development of partially exposed resists for smoothing the LWR. A new negative phenol-based fullerene resist was conclusively presented in this study. The resist offered high sensitivity as well as a high resolution at low exposure doses as compared to the traditional high resolution HSQ resist. The ICP etch rate of IM-MFPT12-8 was revealed to be 0.97 nm/s for SF_6/CHF_3 chemistry.

A positive tone fullerene derivate resist containing the acid labile groups tert-butyl acetate (tBAC) and (tBOC), has also been reported in literature.[51] The sensitivity of the resist was found to lie in the range

of 100-150 μC/cm² and isolated lines as small as 20 nm were successfully patterned. Thus, fullerene comprising materials have emerged as a new high-resolution class of resists.

3.4 Methacrylate Bases Resists

PMMA was the first resist of the methacrylate family and also the earliest EBL resist to be developed.[52] This family of resists consist of a methacrylate backbone ($CH_2CHCO_2CH_3$) and are usually used as positive resists. However, upon elevating the electron dose the resist tone can be reversed into negative. PMMA is still regarded as the standard high-resolution resist and is the most widely used EBL resist. Lines as small as sub-5 nm have been resolved in PMMA by megasonic-assisted development[53] or cold temperature.[54] The other renowned resist of the same family is ZEP, which is a 1:1 copolymer of α-chloro methacrylate and methyl styrene. The high sensitivity and etch durability, as well as the stability of this resist are prominent.[19, 28] Both the resists mentioned can be commonly developed in organic solvents such as MIBK, xylene based, amyl acetate, hexyle acetates and IPA:DI. Methacrylate-based resists offer good lithographic outcomes with ease of handling and hence both compounds have established themselves as mainstay electron beam resists.

During the last 5 years, two new resists with a methacrylate backbone have been reported: SML (EM Resist Ltd., United Kingdom) and chemically semi-amplified resist 62 (CSAR 62) (Allresist GmbH, Germany). The complete chemical structures of both these resists have been withheld, however the presence of a methacrylate group in SML and CSAR 62 has been reported.[10,56] CSAR 62 is a CAR consisting of the copolymer of α-chloro methacrylate and methyl styrene in anisole, much like ZEP. However, unlike ZEP this resist includes additives to enhance its sensitivity, hence semi-chemically amplified.[55] In a very initial study of CSAR 62, its parameters have been compared with those of ZEP and PMMA resists. For the contrast-sensitivity measurement, CSAR was developed using amyl acetate, which is the standard ZED N50 developer of a ZEP resist, o-xylene as well as using a combination of both solvents. The contrast curves plots generated at 100 kV under various conditions are illustrated in Figure 15.

Developing CSAR 62 with amyl acetate gave the highest contrast value of 5.2, as seen in Figure 15(b), however a large amount of resist residues were observed even after the clearance dose. On the other hand, the use of o-xylene developer reduced the residues but at the expense of contrast. The o-xylene dip after developing in amyl acetate gave a contrast (γ) and sensitivity (S) very similar to that of ZEP resist ($\gamma_{ZEP} = 4.18$, S_{ZEP} = 180 μC/cm2 and γ_{CSAR62} = 4.77, S_{CSAR62} = 172 μC/cm2). The ultimate resolution of this resist was presented by another group using a 180 nm thick CSAR 62 resist where lines approximately 10 nm wide were resolved with a pitch of 100 nm, as evident in Figure 15.[57] They also studied the etch rate of the resist with CF_4/O_2 plasma, and an etch rate of 100 nm/min was revealed.

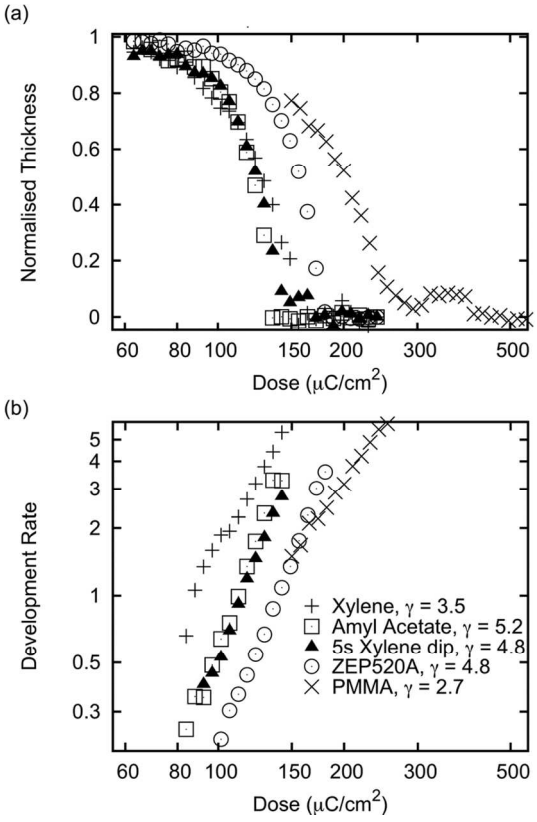


Figure 15. Contrast plots for (+) CSAR 62 developed using o-xylene, (□) CSAR 62 developed using amyl acetate, (▲) CSAR 62 developed using amyl acetate followed by a 5 s dip in o-xylene, (○) ZEP 520A, and (×) PMMA. (a) The normalised remaining resist thickness vs log dose, (b) log development rate plotted against log dose. The contrast, γ, for each resist is also shown.[56]

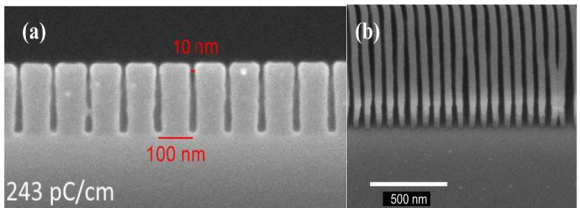


Figure 16. SEM images showing (a) the critical resolution of a 180 nm thick CSAR 62 resist, (b) 200 nm thick CSAR 62 resist image showing 75 nm period lines, some of which show signs of collapse.[56,57]

SML is also an organic, positive toned EBL resist. Initial works on this resist involve lithographic comparisons with PMMA and ZEP resists.[8,58] It was found in a study that SML shows the best contrast-sensitivity trade-off with 7:3 IPA:DI water developer, like PMMA.[58] Contrast curves of 300 nm thick SML resist obtained at 10 kV voltage, in comparison with those of PMMA and ZEP resists, are shown in Figure 17.[10] It is to be noted that ZEP resist was developed in ZED-N50 developer and hence, gave a very high sensitivity of 21 μC/cm2. It is apparent from Figure 17 that the sensitivity of SML is poorest amongst the three. However, it shows a very high contrast of 12, which is similar or even slightly higher than that of the high-resolution PMMA and ZEP resists.[10]

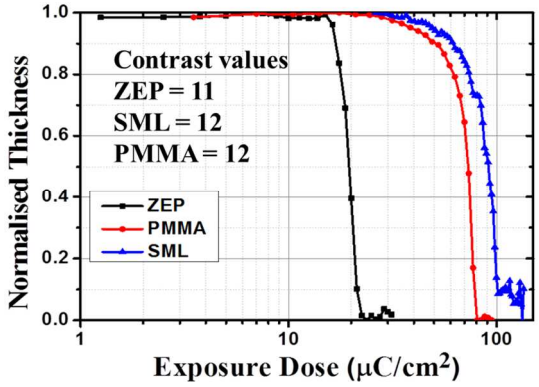


Figure 17: SML 300 compared to ZEP and PMMA resists of 300 nm thickness along with the contrast values.[10]

Lithographic evaluation of the resist shows that high resolution could be achieved in SML with ~15 nm half pitch (Figure 18 (a)). The smallest linewidth resolved in SML is 5 nm and that in ZEP is 7 nm, which are till date the smallest features resolved in both the resists (Figures 18 (d) and (e)). The SML resist also exhibits efficient single layer metal lift-off property. FTIR characterizations have shown that the structural changes occurring in SML polymer after electron exposure are similar to that of PMMA and ZEP resist.[8] The FTIR evaluations revealed that SML is a methyl acrylate based resist and thus, the structural changes upon electron irradiation is bound to be similar such as, increase in unsaturation and alteration in acrylate groups in SML and ZEP polymer chain after electron beam exposure were also revealed.[8] The etching characteristic was compared to that of ZEP with SF_6/C_4F_8 gases chemistry. The initial etch rate of SML was found to be 17 nm/min for 60 s (the one of ZEP was 27 nm/min), and as the etch time increased, the etch rate increased gradually.[10] However, the increased etch rate was comparable to that of ZEP resist. Since, ZEP is also well known for its high etch resistance, it can be said that SML is also a very good candidate as a hardmask during dry etching.[10]

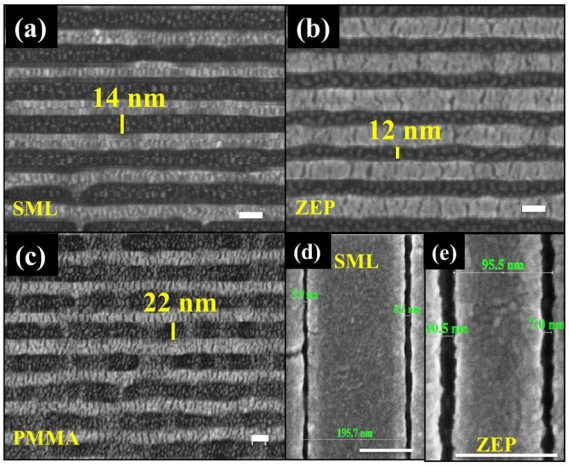


Figure 18: High resolution gratings with 30 nm pitch size on (a) SML 50 developed in 7:3 IPA:water developer, (b) ZEP developed in ZED-N50 and (c) PMMA developed in 7:3 IPA:water (20 nm scale bar). Images (d) and (e) show the smallest linewidths achieved in SML 50 and ZEP, respectively (100 nm scale bar).[10]

Acknowledging the high sensitivity and etch resistance of ZEP resist, a group developed a range of positive resists containing acrylic, chlorine containing monomer (acrylate A) and an acrylic monomer having aromatic side-groups (acrylate B).[55] Copolymers of different compositions of acrylate A and B were synthesized and their lithographic quality was evaluated comparing to that of ZEP and PMMA. Table 4 describes the clearance dose, contrasts as well as the molecular weights of the different copolymers.[59] The mass fraction of acrylate A ranges from 37 to 63 % in the

different copolymers. Evidently, the most sensitive resist is ZEP and Copolymer 5 has similar sensitivity with 30 kV electron beam. The sensitivity is seen to be dependent on the mass fraction of acrylate A, i. e. the clearance dose increases as the mass fractions differs away from 40 wt.%. RIE etch tests of Copolymer 5 revealed its etch resistance similar to that of ZEP. Lithographic evaluation showed that Copolymers 4 and 5 can produce nanometre sized features down to 29 nm. The pinnacle resolution was observed with Copolymer 4 as seen in Figure 19 (a). Figure 19 (b) shows Ti/Au 35 nm gratings attained by lift-off method from a 100 nm thick copolymer 5 (mr-Pos EBR) resist pattern.

Table 4. Molecular weight distributions of the investigated resist materials and the sensitivity and contrast data obtained at 30 kV acceleration voltage.[59]

Resist Material	Molecular weights (g/mol)		Mass fraction of acrylate A (wt.%)	Dose-to-clear ($\mu C/cm^2$)	Contrast γ
	M_n	M_w			
Copolymer 1	90500	160800	52	306	4.0
Copolymer 2	57400	94500	49	217	4.0
Copolymer 3	59200	92900	63	>450	3.7
Copolymer 4	78500	137700	44	90	3.6
Copolymer 5	80900	134200	40	74	3.9
Copolymer 5 (100 kV)	80900	134200	40	340	3.0
Copolymer 6	84700	136100	46	109	3.2
Copolymer 7	32900	66200	37	124	2.8
ZEP 520A	30500	67000	50	>60	-
495 PMMA	-	495000	-	146	6.1

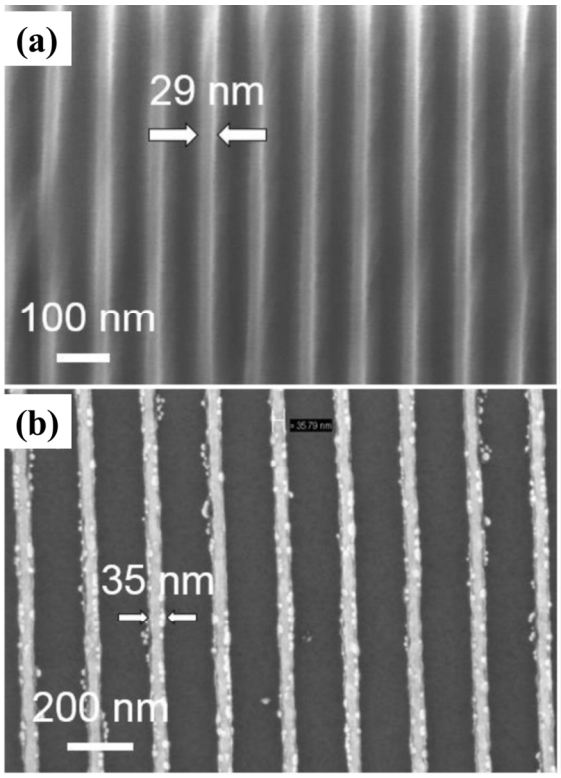


Figure 19: (a) Highest resolution resist pattern obtained in Copolymer 4, 29 nm with a period of 100 nm (LER: 5.9 nm) and (b) 35 nm wide Ti/Au lines obtained via lift-off from mr-Pos EBR resist.[59]

3.5 Inorganic Resists

In comparison to organic resists, inorganic resists generally possess higher contrast and better etch resistance due to their chemical structure, but invariably suffer a reduced sensitivity. The most efficient resist, which has stanchly maintained its high performance, is HSQ. HSQ is the smallest member of the polyhedral oligosilsesquioxane (POSS, trademarked by Hybrid Plastics) family, and has a cubic structure ($HSiO_{3/2}$).[60] On electron beam exposure, the cubic HSQ molecules open and cross-link, forming network structures.[61] HSQ has demonstrated a linewidth resolution of 7 nm, with a pitch size of 14 nm, at a dose of nearly 1 mC/cm (30 kV)[62] and approximately 5 nm width with 40 nm pitch (10 kV).[13] 6 nm isolated lines and 7 nm dense lines at doses of 5.5 and 33 mC/cm^2 respectively (100 kV), have also been reported previously.[63] Nevertheless, due to its sensitivity issues and short shelf-life, HSQ is often troublesome to work with. Therefore, newer inorganic resists with silsesquioxane moieties and others containing metal fragments have emerged.

In 2007 two negative, inorganic resists consisting of hafnium and zirconium oxide sulphates, known as $HafSO_x$ and $ZircSO_x$ respectively, were reported.[64] These materials are atomically very dense thus sensitizing the resists and due to their metallic nature they can be good candidates during ion etches.[65] Resist solutions were prepared by combining $HfOCl_2$(aq) or $ZrOCl_2$(aq) with a mixture of H_2SO_4, H_2O_2 and 18 MΩ purified water to give metal:sulphate ratios of 1:0.5 and 1:0.7. The resists were spin-coated onto Si to achieve 35 nm thin films. The contrast curves and high-resolution performance of the resists were evaluated using 30 kV. Figure 18 presents the contrasts curves of the two metal sulphate resist developed with TMAH ($HfOCl_2$ = 90 s and $ZrOCl_2$ = 240 s). Figure 18(a) shows the contrast curves for $HafSO_x$ and $ZircSO_x$ having a metal:sulphate ratio of 1:0.55 and 1:0.5, respectively. The sensitivity of $HafSO_x$ was determined to be 21 μC/cm² with a contrast of 2.5, whereas that of $ZircSO_x$ was 7.6 μC/cm² with a contrast of 2.6. For an inorganic resist with no chemical amplification the sensitivity of both the resists is praiseworthy. Figure 20(b) shows a contrast-sensitivity plot of $ZircSO_x$ having a metal:sulphate ratio of 1:0.7. The sensitivity can be observed to decrease by a factor of 36 relative to its lower sulphate formulation, but with an improving contrast value of up to 5.2. In this study the sensitivity of the resist was correlated to the electron density of the resist polymer. The electron density was measured from the critical angle X-ray reflectivity measurements and was found to be 1.9 mol e^-/cm³ for $HafSO_x$ and 1.5 mol e^-/cm³ for $ZircSO_x$, and for comparison 0.64 mol e^-/cm³ for PMMA. The Bethe equation (2) states that the stopping power for an electron in a solid is directly proportional to the electron density of the solid $N_e = N_A Z_{eff}/A_{eff}$, where N_A is the Avogadro's number.[66] Thus, from the electron densities values measured, the new resists were observed to absorb the energy of the incident electrons more effectively than PMMA. This, in turn, will improve their sensitivity as compared to PMMA. In addition, the unwanted exposure of the resists due to the backward scattering of the incident electrons will also be reduced. The reaction mechanism of HafSOx correlated to its chemistry was shown by a group by energy-dispersive X-ray spectroscopy.[67] The pre-bake treatment of HafSOx drives to densification of HafSOx thin film. Upon exposure to electron beam, the peroxide moiety is decomposed inducing condensation reactions that makes the resist insoluble in the developer solution (25% TMAH). During development, the mobile sulphate species is replaced by –OH, which prepares for additional insolubleness of the resist.

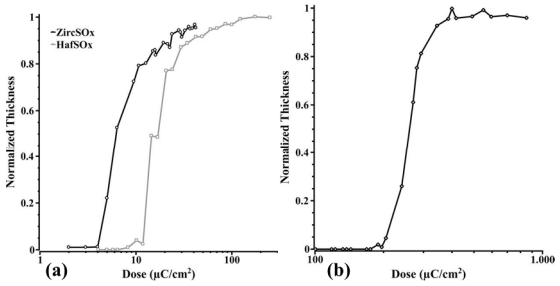


Figure 20. (a) Contrast curves of $ZircSO_x$ and $HafSO_x$ developed in TMAH and having metal: sulphate ratio of 1: 0.55 and 1: 0.5, respectively. (b) Contrast curve of $ZircSO_x$ having a metal: sulphate ratio of 1:0.7.[64]

The resolution of $ZircSO_x$ resist was evaluated by exposing line patterns on Si. The highest resolution achieved was a 16 nm isolated line, from a 1:0.5 ratio of $ZircSO_x$ and sulphate as shown in Figure 21(a), as well as a dense grating with line widths of 28 nm and a period of 100 nm, as shown in Figure 21(b). Isolated and dense gratings with 1:0.7 ratio of $ZircSO_x$ and sulphate are illustrated in Figures 21(c) and (d), respectively. The reaction mechanism of this resist during exposure is believed to be similar to that of HafSOx.[67,68] The obvious difference between the two types of gratings is the LER, which appears higher for structures prepared with the 1:0.5 resist mixtures. The 3σ line width roughness values calculated for isolated and dense lines were 3.4 and 6.4 nm, respectively. In comparison, the 3σ values with the 1:0.7 resist mixtures were 1.9 nm for an isolated line and 2.1 nm for a dense grating. For the line shown in Figure 19(a), a dose of 112 μC/cm² was required, whereas the isolated line shown Figure 21(c) was achieved with a dose of 999 μC/cm². Thus, by increasing the sulphate concentration the quality of the structures is improved, but at the cost of reduced sensitivity. The etch rates of $HafSO_x$ and $ZircSO_x$ were determined as 2.2 nm/min and 2.9 nm/min respectively, by reactive CHF_3 plasma etching.

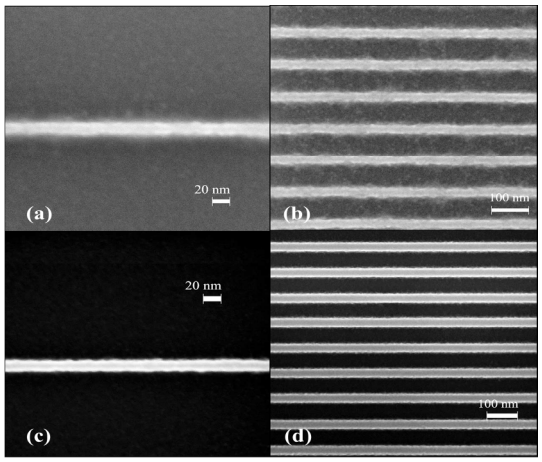


Figure 21. SEM images of isolated lines and dense gratings in $ZircSO_x$: (a) 16 nm isolated line in a 1:0.5 ratio of $ZircSO_x$ and sulphate at a dose of 112 μC/cm², (b) 28 nm lines in a 100 nm period in a 1:0.5 ratio of $ZircSO_x$ and sulphate at a dose of 50 μC/cm², (c) 15 nm isolated line in a 1:0.7 ratio of $ZircSO_x$ and sulphate at a dose of 999 μC/cm² and (d) 36 nm lines at a 100 nm period in a 1:0.7 ratio of $ZircSO_x$ and sulphate at a dose of 810 μC/cm².[64]

Thus, these resists exhibit high-resolution structures and high sensitivity comparable to that of several positive resists[10,55] with lower roughness values and a good etch durability. Significantly, the sensitivity of these resists is very high when compared to HSQ.

Most of the non-organic resists are characterised by high etch resistance and also offer good resolution. In the following contribution, a spin-on hybrid resit system is exhibited, which on electron beam radiation turns onto an inorganic alumina, i.e. a hardmask.[69] Tests showed etch selectivity towards Si in excess of 100:1, which is only comparable to that of metallic hardmasks. The resist is referred to as PhSiAl, abbreviation of Phenyl Silane and Aluminium-tri-sec-butoxide. It was synthesized by a sol-gel method by continuously stirring aluminium-tri- sec-butoxide (97%, Aldrich) with acetic acidin ratio of 1:0.05. After 1 h, 20% trimethoxyphenyl-silane (≥95.0%, Aldrich) was added to it and stirred at 80 °C. The resulting solution was spun on Si substrates, variably diluted with ethanol to give resist film thicknesses from 30 nm to 1 μm. Contrast curves were not available for the resist, but the optimum dose mentioned for this resist is 800 μC/cm² at 30 kV for dose matrix experiments[64], indicating that the resist sensitivity is in the vicinity of HSQ sensitivity. Depending on the choice of developer, when developed in buffered oxide etch (BOE) it can be a positive resist, whereas when developed in HCl and IPA mixture, it can act as a negative resist. The structural changes in the resist film after irradiation was determined by FTIR measurements on resist films exposed to UV light and X-rays, illustrated in Figure 22.[70]

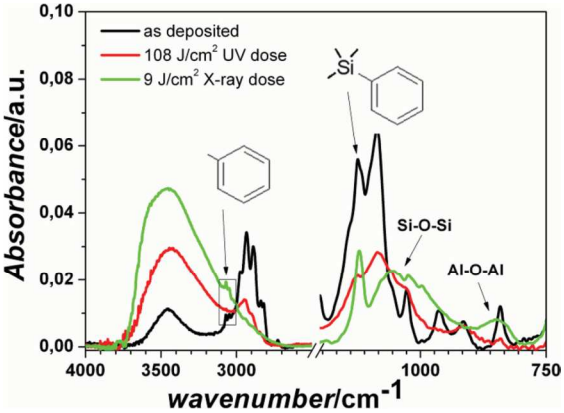


Figure 22. FTIR spectra of the alumina-based resist films before and after exposure to a UV dose of 108 J cm –2 and an X-ray dose of 9 J cm –2.[70]

It is seen from the FTIR plot in Figure 22 that on exposure, the aromatic rings in the resist are shrivelled after exposure, confirming the degradation of organic network. Rise of the peaks near 3400 cm-1 confirms hydrolysis reaction of alkoxides, which happens due to increase in inorganic network. It is also confirmed by the Si-O-Si and Al-O-Al absorptions visible in the plot.[70]

Lithographic assessments were carried out at 3 kV and evince very high resolution structures as seen in Figure 23. Figure 23 (a) shows array of diminutive resist gratings and an inset showing the 20 nm dimension of one of the lines and the highest resolution reported in this article is 11 nm grating. Similar structures were dry etched into Si by using SF_6, C_4F_8 and Ar gas mixture[69] and the resist etch rate was found to be 2.67 nm/min with this gas mixture. Figure 23 (b), (c) and (d) show SEM images of gratings and pillars etched down to 300-400 nm depth using the resist hardmask. This calibre is remarkable because ~40 nm thick resist solely is able to work as an efficient hardmask for high-resolution lithography.

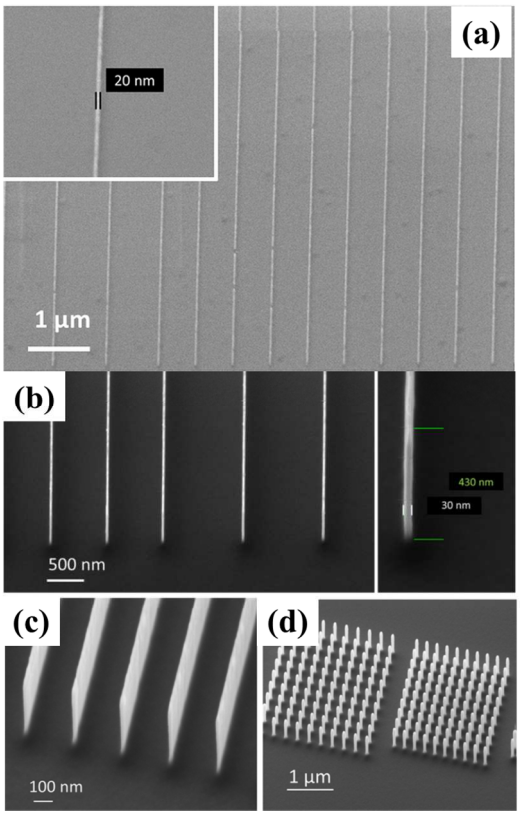


Figure 23: (a) Examples of lithography results achieved with optimized EBL parameters (3 keV acceleration voltage, 200–250 µC cm-2 exposure dose, 2 min at 120 °C PEB (b) Images of the same sample, with lines of 30 and 20 nm etched down to a depth of more than 400 nm; (c) and (d) images of the same sample, with 20 nm lines and 50 nm diameter pillars etched down to 350 nm.[69]

3.6 Miscellaneous Resists

There is a variety of commercial resists available with different lithographic parameters. For instance, incorporating metal into a material can boost the etch resistance of a resist. Metal salts of methacrylic acids (MAA), e.g. Pb, Ba, Ca and Sr, have been incorporated into PMMA resists.[71] The sensitivity of PMMA was improved by a factor of 3 by the best-suited metal, i.e. Pb. Additionally, metal-impregnated PMMA resists better withstand acidic and basic etch chemistries compared to PMMA alone.

Along with the resist parameters, one major concern is the environmental and human impact of chemicals used in lithography processes. Keeping this point in mind, water-soluble resists have been reported for EBL technology that can help reduce the carbon footprint. In the next section, two different water-soluble resists are discussed.

With the purpose of achieving a creditable etch durability whilst lessening the environment impact, poly (sodium 4-styrenesulphonate) (PSS) was recently employed as an EBL resist.[72] Sodium not only has a positive effect on the etch resistance but, due to the ionic nature of PSS, it can also be dissolved and developed in water. The resist solution was prepared by dissolving 70 kg/mol PPS (Sigma Aldrich) in DI water to make a 7 wt/vol% solution, which produced a thin resist film of approximately 180 nm. The film was then baked and exposed with a 20 keV beam to procure contrast curves and high-resolution patterns. Post exposure, the resist was developed with DI water for 10 s at room temperature. Figure 24 illustrates the contrast curve for the PSS resist along with its chemical structure and the high resolution patterning by EBL in PSS.

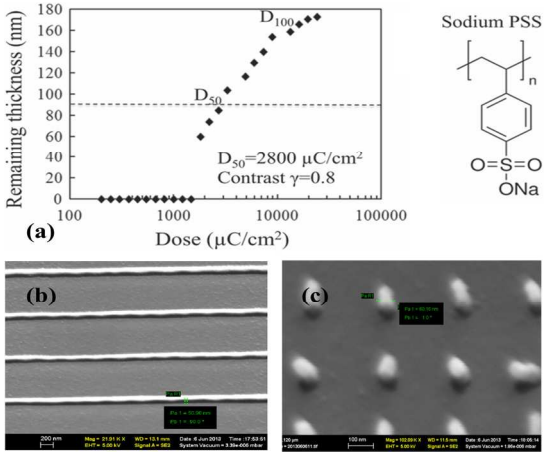


Figure 24. (a) Contrast curve of the water-soluble PSS resist, (b) SEM image showing a line array with a line width ~60 nm (narrower lines were found to have collapsed). (c) SEM images showing arrays of pillars with a mean diameter of 60 nm.[72]

From the contrast curve in Figure 24(a), the sensitivity of 2800 µC/cm² is poor, as is the contrast of 0.8. However, the authors suggest that the use of higher molecular weight PSS to improve its sensitivity drastically, since for the cross-linking polymer chains the exposure dose is found to be inversely proportional to its molecular weight.[73] However, the resist would not be ideal for high-resolution patterning as the EBL process would be extremely sluggish. For testing the etch resistance, an O2 plasma RIE test (20 sccm O2, 20 mTorr, 20 W RF power) of PSS was compared to PMMA. PSS

showed 17 times higher etch resistance than PMMA, and 6 times higher than SU-8 and polystyrene resists (from literature), which have similar sensitivity and contrast to that of PSS. Since PSS contains metal sodium, higher tolerance to dry etching is expected as compared to PMMA. The etch test with CF_4 gas (20 sccm CF_4, 20 mTorr, 100 W RF power, room temperature) revealed that the selectivity relative to PMMA was only 3.5 times higher. This low selectivity with CF_4 is thought to be because of the low percentage of sodium in PSS. Finally, to assess the resolution of this poorly sensitive resist, high-resolution gratings and pillars were exposed on a 180 nm thick resist film. The resist was not good for dense exposures and gratings with 100 nm spacing. The critical dimensions achieved were 60 nm linewidth with 400 nm pitch (Figure 24(b)) and pillars with a mean diameter of 60 nm with 300 nm pitch (Figure 20(c)), which is quite reasonable for a 180 nm thick resist film. However, gratings with lower spacing and pillars smaller than 40 nm in diameter collapsed due to the capillary force during drying after water development. Additionally, the authors demonstrated a metal lift-off of 2 keV exposed structures by DI water. To conclude, although PSS is not a model resist for fast and dense critical patterning, it definitely exhibits an excellent etch durability. Moreover, the fact that it can be developed and further processed with water makes it environmentally friendly and less hazardous for humans.

Engineers in Tufts University, US, have developed an apparent 'green alternative' resist.[74] Silk, a biologically fabricated material, has long been enjoyed as a luxurious and beautiful fabric, yet it is tougher than most of the synthetic fibres currently present in the market.[75] For this reason, silk proteins have been utilised in recent years in areas as diverse as photonics, electronics, drug delivery and bio-scaffolds.[75,76,77] Recently, engineers in Tufts University expanded the possibility of using silk as a nanofabrication material. They showed that EBL was able to change the protein structure upon irradiation thus making it a candidate for EBL resists. This report demonstrated that the silk resist could be used as either a negative (amorphous silk form) or positive (crystalline silk form) resist. Moreover, silk can be converted into 'functional resists' by doping the resist solutions with organic, inorganic or even biologically active materials. In this segment, silk resist preparation, sensitivity values and resolution will be discussed.

Resist solutions were produced by boiling silk cocoons in sodium carbonate solution to obtain fibres, which were then dried overnight. The dried fibres were subsequently dissolved in 9 M lithium bromide resulting in a ~7 % aqueous resist solution of silk fibroin. The resist was then spun onto a substrate to give a 200 nm thick silk layer; the thickness of which could be controlled by the spin speed. In order to yield a negative resist, after spin coating the intermolecular crosslinking within the resist was achieved by either exposing the substrates to water vapour for > 12 h or by dipping in methanol for 60 s, followed by exposure to water vapour for 2 h. Both resists were typically exposed with high-energy beams of 100 and 125 keV. The development of the resists was done by simple immersion in DI water for 60 s followed by drying.

The minimum doses required to fabricate nanostructures at 100 kV were reported. In the case of the positive resist, the dose required to fabricate nanoscale features was 2250 μC/cm² and that for the negative form was 25,000 μC/cm². These values are 2.5 times higher than that required by PMMA at 100 keV.[78] Figure 21 illustrates photonic crystals having various spacing obtained by EBL exposure of both varieties of the silk resist.

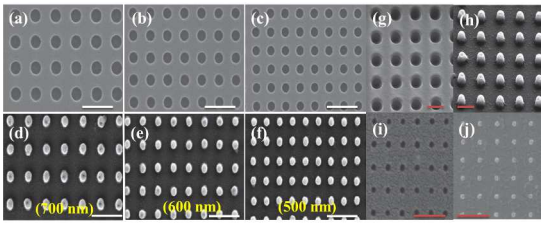


Figure 25. (a-c) SEM images of photonic crystals fabricated with positive silk whereas (d-f) are with negative silk; with a lattice constant or periodicity for (a) and (d) of 700 nm; for (b) and (e) 600 nm; for (c) and (f) 500 nm; (g) and (h) are 200 nm diameter holes and pillars, respectively;(i) and (j) are highest resolution 30 nm holes and pillars patterned by the silk resist.[74]

Evident from the SEM images shown in Figure 21 is that the 'green' resist is capable of fabricating nanostructures competently. Images from Figures 25(a-c) are the photonic crystals fabricated with a positive silk resist, whereas Figures 25(d-f) are produced with a negative silk resist, with lattice constant (periodicity) of 700 nm (Figures 25(a and d)), 600 nm (Figures 25(b and e)) and 500 nm (Figures 25(c and f)). The diameters of the crystals were designed to be 200 nm; and from the SEM images in Figures 25(g) and (h) it can be seen that there is no widening or narrowing of the structures, thus suggesting that the resist is capable of good lithography. Figures 25(i) and (j) illustrate the highest resolution obtainable with the two resists, that is, 30 nm holes and pillars with positive and

negative resists, respectively. Furthermore, the authors suggested that these resolution limits could be pushed further by tuning the molecular weight of the silk solution or by adding other biomolecules, for instance, microbial transglutaminase or mushroom tyrosinase. Thus, the possibility of using a biomaterial, silk, for EBL process was successfully demonstrated in this study. Moreover, another advantage of using silk, highlighted by them, is the ease of functionalising them to act like a unique class of bio-active resist. To conduct their tests, the silk solutions were doped with quantum dots, green fluorescent proteins (GFP) or horseradish peroxidase enzyme (HRP). They were able to validate the fabrication of high-quality nanoscale optics like quantum dots (inorganic) or GFPs (organic) that enhanced the fluorescent signalling from the silk devices. Dry etching was perform[79] Etch rate with O_2 and C_4F_8 gases constituted to be 9.10 nm/s. Although in its early stage of development, this is a new, eco-friendly resist which minimises the need to work with toxic chemicals and is potentially a step towards establishing a green cleanroom process.

4 ADVANCED LITHOGRAPHY

Top-down fabrication of the devices has, over the years, improved tremendously. Presently, the trend has diverted to three dimensional (3D) device fabrication.[80] 3D devices find applications in a large number of fields including photonic crystals, biosensors and metamaterials.[80,81,82] Especially the devices that are fabricated with the EBL technique require multiple steps and precise alignment of different layers.[83,84,85] Besides the EBL method, advances in appliances employed in device fabrications are also being upgraded continuously and form the so-called next generation lithography (NGL) systems, which are briefly described earlier in section 1.2. Few of the charged particle NGL systems are discussed next.

Proton beam lithography or proton beam writing (PBW) is one of the techniques that are used for nanofabrication. Reports of utilising this technique for high aspect ratio and 3D fabrication are published, wherein multiple proton beams with different energies (and at different incident angles) are used for nanofabrication.[86,87]

Helium ion beam lithography (HIBL) is also an example of a NGL process, which has successfully patterned not only non-traditional semiconductor materials but is capable of also directly patterning metals. It possesses a spot size down to 0.75 nm at an accelerating voltage of 30 kV, thus routinely enabling resolution down to 0.35 nm.[88] Moreover, due to the fact that ions are much heavier than electrons, they experience less scattering in the resist and the substrate and the proximity effect experienced is almost negligible. They provide also faster resist exposure (higher sensitivity), potentially enabling resolution beyond that of EBL.[89] Apart from being able to pattern resists down to 6 nm, helium ion beam also provides enhanced quality imaging as a microscope.[88] A very recent study demonstrated that HIBL was able to pattern a fullerene derivative resist with sensitivity of almost three order magnitude more than EBL.[90] Thus, due to the nature of ions, writing-times can be immensely reduced with this NGL technique.

EBL is well known for achieving critical resolutions with much ease but suffering from low throughput. In order to increase the throughput of this technique, multiple electron beam (multibeam) approach is currently under evaluation as an NGL tool.[91] The two major applications of such systems are direct-write on wafer level and mask-making.[92] There are various tactics that are considered for lithography like multiple columns, in which each beam source can have micro (for low voltage beams, 1-2 keV[93]) or mini columns (1-50 keV beams[94]). Other strategies are using a single column with multiple electron beam sources or distributed multiple beams where several beam sources are distributed over a portion or the entire area of the wafer.[92]

The next generation lithography (NGL) techniques are, however, relatively expensive and not mature enough for widespread application. Their use for mass-production seems at the moment highly unlikely. Therefore, it is necessary to better understand these top-down techniques as well as to improve the existing techniques for nanoscale fabrication. Bottom-up techniques like directed self-assembly of block copolymers are also a promising technology favouring the progress of nanofabrication.

5 SUMMARY

Lithography is a vital element of nanoscale fabrication. In the last decade, the critical dimension of microelectronic devices has dramatically reduced while circuit complexity has increased.

Consequently, the requirement for microfabrication technology reaches into the nanometre regimen. In order to meet these requirements, the need has arisen for finer pattern generation and lithography systems with superior performance specifications. Advances in EBL systems have led to reduction in the beam size diameter down to 1-2 nm. However, achieving feature sizes equivalent to this small probe size remains difficult mainly due to the issues with resist morphologies and lithographic processes. To obtain the best outcome from any EBL process, the tool, the resist parameters and the overall lithography process must be optimised for good outcomes. All the resist parameters collectively described in Section 2 determine the quality of a resist. Nevertheless, it is not always that a single resist will exhibit all the parameters commendably, *i.e.* the resist may have a high resolution but may suffer low sensitivity value or etch durability. Due to the growing interest of lithography community to attain high performance lithography, there is a high motivation to develop novel EBL resists. This review summarises recent developments in EBL resists and compartmentalizes them into various families and expressing their various functions and merits. The resist families are classified according to their chemical compositions.

Firstly, the chemically amplified resists (CARS) were discussed and it is evident from the new, as well as, early reports that this division of resists are extremely sensitive to electron beam. State-of-the-art CARS exhibit electron sensitivity from 7 $\mu C/cm^2$ up to 200-300 $\mu C/cm^2$ and are able to offer high resolution structures down to 15 nm. The main issue with CARS is photo acid generation, not only during exposure but also in the interval between spinning the resist and exposure. This issue has been countered by casting a protective layer over the resist, which does not affect the sensitivity of the resist and protects it from unwanted alterations in the composition due to acid diffusion. Thus, by protecting the resists their stability is improved, which can lead to enhanced sensitivity and also ease patterning that requires mix-and-match lithography wherein one substrate requires two different patterning procedures with different or same tools. By controlling the acid diffusion within the resist after electron exposure and exploiting the advantage of high sensitivity of CARS, they project as worthy next-generation lithography resists. Conversely, in order to eradicate the additional unwanted acid-diffusion concerns of the CARS completely, non-CARS resists have been formulated. Such resists include mainly a sulphonium salt portion that will allow them to exhibit high sensitivity.

The infusion of a fullerene moiety, C_{60}, into various polymer blends leads to beneficial resist characteristics like high sensitivity and resolution, high etch resistance, low line width roughness and compatibility with industrial processing. Such materials can account for newer class of resists. In order to gain the best productivity from such resists, exploring more about their exposure mechanism, better understanding the role of C_{60} in the whole EBL process and tuning resists parameters should be undertaken.

Methacrylate based resists are one of the generally favoured families of resists, due to the ease of handling and simplicity in their chemical formulation and exposure mechanism as compared to CARS or fullerene based resists. Conventional resists like PMMA, ZEP or SAL (Shipley Advanced Lithography) belong to this family of resists. Newer products from this family, such as SML or CSAR are modified to either have increased sensitivity, etch durability or high resolution.

The highest resolution of ~5 nm features has been achieved by EBL using inorganic resists.[13] The widespread use of these resists is usually hindered due to their low sensitivity. HSQ is one of the most commercially and scientifically successful EBL resist, but it displays relatively low sensitivity. Therefore, inorganic resists have been recently prepared, which exhibit higher sensitivity while maintaining high resolution. Most of these new inorganic resists contain metal components such as hafnium, zirconium or aluminium.[64] These resist do not only break the sensitivity limitations of inorganic resists but are also compatible for nanofabrication processes. They can be deposited easily from their aqueous solutions and also form even thickness films on substrates. A recent study reported use of colloidal nanocrystals, ZrO_2 and HfO_2 suspended in hexane, used as resists for plasma powered lithography.[95] Wherein, hardmasks were pressed against the substrate but the exposure was caused by plasma power in etcher tool. This study supports the concept that the trend in inorganic resists seems to incline towards resists that are able to metallize after irradiation. Thus, eradicating process steps like metallization and lift-off.

Traditional EBL resists are mainly formulated with a view to gain maximum throughput over a fast processing period, often leading to the use of

hazardous chemicals for processing, or even the resists themselves can be perilous in nature. Recently, benign resist materials have also been developed like PSS, as described in miscellaneous resists section. Other resist that grasps this group are polyanilines water-based conducting EBL resists.[96] Biomaterials such as silk fibres have also been demonstrated as potential eco-friendly EBL resists.[74,97] Research towards non-hazardous and environment-friendly resists and developers may, in the future, become an important trend in developing new materials for nanofabrication.

In conclusion, in the past few decades, many materials have been suggested as potential EBL resists. High sensitivity and resolution together with good etch resistance continually remain the most desirable characteristics of EBL resists. The different classes of resists detailed in this report highlight the progress currently being made in the development of resist materials. With the EBL systems reaching their maturity in term of resolution, few NGL techniques are also reported in this paper. Table 5 summarises all the resists reported hitherto along with their family type, tones, developers, sensitivity and contrast values obtained at specific electron beam voltages and the critical dimension achieved by the resist. It is to be noted that in the cases where two or more resist derivatives were testified, only the ones with superlative performance are tabulated in table 5.

Table 5. Summary of the electron beam resists based on their family, tone; positive (P) or negative (N), developers, sensitivity, contrast, electron beam voltage, dry etch conditions, etch rates, critical dimension (CD) and the dense pattern features attained in the resists

Number	Name	Family	Tone	Developer	Sensitivity ($\mu C/cm^2$)	Contrast (γ)	EBL Voltage kV	Etching Gases	Etch Rate nm/min	CD (nm)	Dense Patterns Pitch/CD (nm)
1	Poly(GMA-co-MMA-co-TPSMA)[32]	CARS	N	7:3 IPA:DI water	125	-	100	CF_4	40	15	20/19
2	40XT/PEDOT-PSS[35]	CARS	P	AZ®7 26MIF	7	7	20	-	-	80	70/90
3	MAPDST-MMA[39]	n-CARS	N	TMAH	2	1.8	20	CHF_3/O_2	~9*	20	40/20
4	P(HEMA-co-MAAEMA)[42]	n-CARS	N	Methanol	0.89	1.2	50	SF_6, Wet HNA	225, 15	125	200/125
5	C_{60}-(P(CMS_{14}-HS))[47]	Fullerene Derivative	N	Acetone	40	-	100	-	-	50	50/50
6	IM-MFP12-8[49]	Fullerene Derivative	N	1:1 Monocholoro-benzene:IPA	43	1.3	20	SF_6/C_4F_8	58	18	50/18
7	CSAR 62[56]	Methacrylate	P	Amyl-acetate	172	5.2	100	CF_4/O_2	100	10	150/75
8	SML[10]	Methacrylate	P	7:3 IPA:DI water	60	9.2	10	$SF_6/C4F_8$	17	15	30/15
9	Mr-Pos EBR (Copolymer 5)[59]	Methacrylate	P	Amyl-acetate	74	3.0	30	SF_6/CF_4	200	29	100/29
10	$HafSO_x$[04]	Inorganic	N	TMAH	21	2.5	30	CHF_3	2.2	9[07]	21/9[07]
11	$ZircSO_x$[64]	Inorganic	N	TMAH	8	2.6	30	CHF_3	2.9	16	100/28
12	PSS[72]	Water-soluble	N	DI water	2,800	0.8	20	O_2	~17**	50	-
13	Silk[74]	Water-soluble	P & N	DI water	2,250 (P) 25,000 (N)	-	100	C_4F_8/O_2	546	30 (dot)	-

AUTHOR INFORMATION

Corresponding Author

* Justin D. Holmes: J.Holmes@ucc.ie

Present Addresses

† Institute of Ion Beam Physics and Material Research, Helmholtz-Zentrum Dresden-Rossendorf, Bautzner Landstraße 400, 01328 Dresden, Germany
On leave of absence from the Institute of Electronics, Bulgarian Academy of Sciences, Sofia. Bulgaria.

ACKNOWLEDGMENT

The authors would like to acknowledge the financial support from Science Foundation Ireland (SFI) under the "Novel Nanowire Structures for Devices" Project (Grant Agreement No. 09-IN1-I2602).

REFERENCES

1. Zhang X., Sun C.; Fang N. Manufacturing at nanoscale: Top-down, bottom-up and system engineering. *J. Nanopart. Res*. **2004**, 6, 125.
2. Brewer G.R, in *Electron-Beam Technology in Microelectronic Fabrication*. Ed. **1980**, pp. 2-56.
3. P.J. Silverman. The Intel lithography roadmap. *Intel Technology Journal*. **2002**, 6, 55.
4. Grigorescu A.E.; Hagen C.W. Resists for sub-20-nm electron beam lithography with a focus on HSQ: state of the art. *Nanotechnology*. **2009**, 20, 292001.
5. Cui Z. *Nanofabrication: principles, capabilities and limits.* Springer: Boston, MA, **2008**.
6. Wi J.-S.; Lee H.-S.; Kim K.-B. Enhanced Development Properties of IPA (Isopropyl Alcohol) on the PMMA Electron Beam Resist. *Electronic Mater. Lett*. **2007**, 3, 1.
7. Pragya Tiwari, A.K. Srivastava, B.Q. Khattak, Suveer Verma, Anuj Upadhyay, A.K. Sinha, Tapas Ganguli, G.S. Lodha, S.K. Deb. Structural modification of poly (methyl methacrylate) due to electron irradiation. *Measurement*, **2014**, 51, 1.
8. Gangnaik A.; Georgiev Y.M.; Holmes J.D. Correlation of lithographic performance of the electron beam resists SML and ZEP with their chemical structure. *J. Vac. Sci. Technol. B*. **2015**, 33, 041601.
9. Yang H.; Jin A.; Luo Q.; Gu C.; Cui Z. Comparative study of e-beam resist processes at different development temperature. *Microelectron. Eng.* **2007**, 84, 1109.
10. Gangnaik A.; Georgiev Y.M.; McCarthy B.; Petkov N.; Djara V.; Holmes J.D. Characterisation of a novel electron beam lithography resist, SML and its comparison to PMMA and ZEP resists *Microelectron. Eng.* **2014**, 123, 126.
11. Wu C. S.; Makiuchi Y.; Chen C. in Lithography, Eds. M. Wang, Intech, Vukovar, **2010**, Chapter 13, pp. 241-266.
12. Chang T.H.P. Proximity effect in electron-beam lithography. *J. Vac. Sci. Technol.* **1975**, 12, 1271.
13. Gangnaik A.S.; Georgiev Y.M.; Collins G.; Holmes J.D. Novel germanium surface modification for sub-10 nm patterning with electron beam lithography and HSQ resist. *J. Vac. Sci. Technol. B.* **2016**, 34, 041603.
14. Yasin S.; Hasko D. G.; Khalid M. N.; Weaver D. J.; Ahmed H. Influence of polymer phase separation on roughness of resist features in UVIII. *J. Vac. Sci. Technol. B.* **2004**, 73, 259.
15. Constantoudis V, Gogolides E, Patsis GP, Tserepi A, Valamontes ES. Characterization and simulation of surface and line-edge roughness in photoresists. J. *Vac. Sci. Technol. B.* **2001**, 19, 2694.
16. Georgiev Y.M.; Henschel W.; Fuchs A.; Kurz H. Surface roughness of hydrogen silsesquioxane as a negative tone electron beam resist. *Vacuum*, **2005**, 77, 117.
17. Küpper D.; Küpper D.; Wahlbrink T.; Henschel W.; Bolten J.; Lemme M.C.; Georgiev Y.M.; Kurz H. Impact of supercritical CO_2 drying on roughness of HSQ e-beam resist. *J. Vac. Sci. Technol. B*, **2006**, 24, 570.
18. Kim J.M.; Hur Y. H.; Jeong J.W.; Nam T.W.; Lee J. H.; Jeon K.; Kim Y. J.; Jung Y. S. Block Copolymer with an Extremely High Block-to-Block Interaction for a Significant Reduction of Line-Edge Fluctuations in Self-Assembled Patterns. *Chem. Mater.* **2016**, 28, 5680.
19. Koshelev K.; Mohammad M.A.; Fito T.; Westra K.L.; Dew S.K.; Stepanova M. Comparison between ZEP and PMMA resists for nanoscale electron beam lithography experimentally and by numerical modelling. *J. Vac. Sci. Technol. B.* **2011**, 29, 306.

20. Yang J.K.; Cord B.; Duan H.; Berggren K.K.; Klingfus J.; Nam S.W.; Kim K.B.; Rooks M.J. Understanding of hydrogen silsesquioxane electron resist for sub-5-nm-half-pitch lithography. *J. Vac. Sci. Techol. B.* **2009**, 27, 6.
21. Chen W.-C.; Lin S.-C.; Dai B.-T.; Tsai M.-S. Chemical Mechanical Polishing of Low-Dielectric-Constant Polymers: Hydrogen Silsesquioxane and Methyl Silsesquioxane. *J. Electrochem. Soc.* **1999**, 146, 3004.
22. Yasin S.; Hasko D.G.; Ahmed H. Comparison of MIBK/IPA and water/IPA as PMMA developers for electron beam nanolithography. *Microelectron. Eng.* **2002**, 61, 745.
23. Tanenbaum D.M.; Lo C.W.; Isaacson M.; Craighead H.G.; Rooks M.J.; Lee K.Y.; Huang W.S.; Chang T.H.P. High resolution electron beam lithography using ZEP-520 and KRS resist at low voltage. *J. Vac. Techol. B.* **1996**, 14, 3829.
24. Nishida T.; Notomi M.; Iga R.; Tamamura T. Quantum Wire Fabrication by E-Beam Elithography Using High-Resolution and HighSensitivity E-Beam Resist ZEP-520. *Jpn. J. Appl. Phys.* **1992**, 31 4508.
25. http://www.allresist.com/ebeamresist-positiv-csar62-alternative-zep
26. Murata M.; Miura T.; Yumoto Y.; Ota T.; Kobayashi E. *Google patents*, Number 5, **1996**, 580, 695.
27. Ito H. IBM J. Chemical amplification resist: History and development within IBM. *Res & Dev.* **1996**, 41, 69.
28. Voigt A.; Heinrich M.; Martin C.; Llobera A.; Rius G.; Gruetzner G.; Perez-Murano F. Improved properties of epoxy nanocomposites for specific applications in the fields of MEMS/NEMS. *Microelectron Eng.* **2007**, 84, 1075.
29. Aktary M.; Jensen M.O.; Westra K.L.; Brett M.J.; Freeman M.R. High-resolution pattern generation using the epoxy novolak SU-8 2000 resist by electron beam lithography. *J. Vac. Sci. Technol. B.* **2003**, 21, L5.
30. Wu H.; Gonsalves K.E. Preparation of a Photoacid Generating Monomer and Its Application in Lithography. *Adv. Funct. Mater.* **2001**, 11, 271.
31. Lawson R.A.; Lee C.T.; Yueh W.; Tolbert L.; Henderson C.L. Epoxide functionalized molecular resists for high resolution electron-beam lithography. *Microelectron. Eng.* **2008**, 85, 959.
32. Yoo J.B.; Park S.-W.; Kang H.N.; Mondkar H.S.; Sohn K.; Kim H.-M.; Kim K.-B.; Lee H. Triphenylsulfonium salt methacrylate bound polymer resist for electron beam lithography. *Polymer*. **2014**, 55, 3599.
33. Nalamasu O.; Reichmanis E.; Hanson J.E.; Kanga R.S.; Heimbrook L.A.; Emerson A.B.F.; Baiocchi A. Effect of post-exposure delay in positive acting chemically amplified resists: An analytical study. *Polym. Eng. Sci.* **1992**, 32, 1565.
34. MacDonald S.A.; Hinsberg W.D.; Wendt H.R.; Clecak N.J.; Willson C.G.; Snyder C.D. Airborne contamination of a chemically amplified resist. 1. Identification of problem. *Chem. Mater.* **1993**, 5, 348.
35. Kofler J.; Schmoltner K.; Klug A.; List-Kratochvil E.J.W. Highly robust electron beam lithography lift-off process using chemically amplified positive tone resist and PEDOT:PSS as a protective coating. *J. Micromech. Microeng.* **2014**, 24, 095010.
36. Postnikov S.V.; Stewart M.D.; Tran H.V.; Nierode M.A.; Medeiros D.R.; Cao T.; Byers J.; Webber S.E.; Wilson C.G. Study of resolution limits due to intrinsic bias in chemically amplified photoresists. *J. Vac. Sci. Technol. B.* **1999**, 17, 3335.
37. Krysak M.; Jung B.; Thompson M.O.; Ober C.K. Investigation of acid diffusion during laser spike annealing with systematically designed photoacid generators. *Proc. SPIE, Advances in Resist Materials and Processing Technology XXIX*. **2012**, 8325, 83250M.
38. Gonsalves K.; Wu H. A Novel Single-Component Negative Resist for DUV and Electron Beam Lithography. *Adv. Mater.* **2001**, 13, 195.
39. Singh V.; Satyanarayana V.S.V.; Sharma S.K.; Ghosh S.; Gonsalves K.E. Towards novel non-chemically amplified (n-CARS) negative resists for electron beam lithography applications. *J. Mater. Chem. C.* **2014**, 2, 2118.
40. Satyanarayana V. S. V.; Kessler F.; Singh V.; Scheffer F. R.; Weibel D. E.; Ghosh S.; Gonsalves K. E. Radiation-sensitive novel polymeric resist materials: Iterative synthesis and their EUV fragmentation studies. *ACS Appl. Mater. Interfaces.* **2014**, 6, 4223.
41. Singh V.; S. V. S. Venkata; B. Nikola; R. I. Morales; S. S. K.; Kessler Felipe; Scheffer F. R.; Weibel D.E.; Ghosh S.; Gonsalves K.E. Performance evaluation of nonchemically amplified negative tone photoresists for e-beam and EUV lithography. *J. Micro/Nanolith. MEMS MOEMS*. **2014**, 13, 043002.

42. Canalejas-Tejero V.; Carrasco S.; Navarro-Villoslada F.; García Fierro J. L.; Capel-Sánchez M. del C.; Moreno-Bondi M.C.; Barrios C.A. Ultrasensitive non-chemically amplified low-contrast negative electron beam lithography resist with dual-tone behaviour. *J. Mater. Chem. C.* **2013**, 25, 1392.
43. Tada T.; Kanayama T. Nanolithography using fullerene films as an electron beam resist. *Jpn. J. Appl. Phys.* **1996**, 35, L63.
44. Manyam J. Novel resist materials for next generation lithography. Ph.D. Thesis, University of Birmingham, Birmingham, UK, **2010**.
45. Gibbons F.P.; Robinson A.P.G.; Palmer R.E.; Manickam M.; Preece J. A. Ultrathin Fullerene Films as High-Resolution Molecular Resists for Low-Voltage Electron-Beam Lithography. *Small*, **2006**, 2, 1003.
46. Okamura H.; Takemura T.; Tsunooka M.; Shirai M. Synthesis of novel c60-containing polymers based on poly(vinyl phenol) and their photo-transformation properties. *Polym. Bull.* **2004**, 52, 381.
47. Okamura H.; Forman D.C.; Ober C.K. C60-containing polymers for electron beam lithography. *Polym. Bull.* **2014**, 71, 2395.
48. Choong H.S.; Kahn F.J. Molecular parameters and lithographic performance of poly(chloromethylstyrene)—a high-performance negative electron resist. *J. Vac. Sci. Technol.* **1981**, 19, 1121.
49. Yang D.X.; Frommhold A.; Xue X.; Palmer R. E.; Robinson A.P.G. Chemically amplified phenolic fullerene electron beam resist. *J. Mater. Chem. C.* **2014**, 2, 1505.
50. Takemoto I.; Fuji Y.; Yoshida I.; Hashimoto K.; Miyagawa T.; Yamaguchi S.; Takahashi K.; Konishi S.; Lee Y. Tailored glass transition of ArF resists for resolution enhancement at sub-50 nm node. *J. Photopolym. Sci. Technol.* **2005**, 18, 399.
51. Manyam J.; Frommhold A.; Yang D.X.; McClelland A.; Manickam M.; Preece J.A.; Palmer R.E.; Robinson A.P.G. Positive-tone chemically amplified fullerene resist. *Proc. SPIE, Advances in Resist Materials and Processing Technology XXIX.* **2012**, 8325, 83251U.
52. Haller I.; Hatzakis M.; Srinivasan R. High-resolution positive resists for electron-beam exposure. *IBM. J. Res. Dev.* **1968**, 12, 251.
53. Küpper D.; Küpper D.; Wahbrink T.; Bolten J.; Lemme M.C.; Georgiev Y.M., Kurz H. Megasonic-assisted development of nanostructures. *J. Vac. Sci. Technol. B.* **2006**, 24, 1827.
54. Hu W.; Bernstein G.H.; Sarveswaran K.; Lieberman M. Low temperature development of PMMA for sub-10-nm electron beam lithography. *IEEE-NANO. Third IEEE Conference.* **2003**, 2, 602.
55. Mohammad M.A.; Koshelev K.; Fito T., Zheng D.A.Z.; Stepanova M.; Dew S. Study of development processes for zep-520 as a high-resolution positive and negative tone electron beam lithography resist. *Jpn. J. Appl. Phys.* **2012**, 51, 06FC05.
56. Stephen T.; Macintyre D.S. Investigation of CSAR 62, a new resist for electron beam lithography. *J. Vac. Sci. Technol. B.* **2014**, 32, 06FJ01.
57. Schirmer M.; Büttner B.; Syrowatka F.; Schmidt G.; Köpnick T.; Kaiser C. Chemical Semi-Amplified positive E-beam Resist (CSAR 62) for highest resolution. *Proc. SPIE, 29th European Mask and Lithography Conference.* **2013**, 88860, 88860D.
58. Mohammad M.A.; Dew S.K.; Stepanova M. SML resist processing for high-aspect-ratio and high-sensitivity electron beam lithography. *Res. Lett.* **2013**, 8, 139.
59. Pfirrmann S.; Voigt A.; Kolander A.; Grützner G.; Lohse Olga.; Harder I.; Guzenko V.A. Towards a novel positive tone resist mr-PosEBR for high resolution electron-beam lithography. *Microelectron. Eng.* **2016**, 155, 67.
60. Hobbs R.G. Semiconductor nanowire fabrication via bottom-up & top-down paradigms. Ph.D. Thesis. University College Cork, Cork, Republic of Ireland. **2011**.
61. Namatsu H.; Takahashi Y.; Yamazaki K.; Yamaguchi T.; Nagase M.; Kurihara K. Three-dimensional siloxane resist for the formation of nanopatterns with minimum linewidth fluctuations. *J. Vac. Sci. Technol. B.* **1998**, 16, 69.
62. Yanga J.K.W.; Berggren K.K. Using high-contrast salty development of hydrogen silsesquioxane for sub-10-nm10-nm half-pitch lithography. *J. Vac. Sci. Technol. B.* **2005** 25, 2025.
63. Grigorescu A.E.; Krogt M.C. van der; Hagen C.W.; Kruit P. 10 nm lines and spaces written in HSQ, using electron beam lithography. *Microelectron. Eng.* **2007**, 84, 822.
64. Stowers J.; Keszler D.A. High resolution, high sensitivity inorganic resists. *Microelectron. Eng.* **2009**, 86, 730.
65. Anderson J. T.; Munsee C. L.; Celia M. Hung; Phung T. M.; Herman G. S.; Johnson D. C.;

Wager J. F.; Keszler D. A. Solution-processed HafSOx and ZircSOx inorganic thin-film dielectrics and nanolaminates. *Adv. Funct. Mater.* **2007**, 17, 2117.
66. Joy D.C.; Luo S. An empirical stopping power relationship for low-energy electrons. *Scanning*. **1989**, 11, 176.
67. Oleksak R.P.; Ruther R. E.; Luo F.; Fairley K. C.; Decker S. R.; Stickle W. F.; Johnson D.W.; Garfunkel E.L.; Herman G. S.; Keszler D. A. Chemical and structural investigation of high-resolution patterning with HafSOx. *ACS Appl. Mater. Interfaces*. **2014**, 6, 2917.
68. Hino, M.; Kurashige, M.; Matsuhashi, H.; Arata, K. The surface structure of sulfated zirconia: Studies of XPS and thermal analysis. *Thermochim. Acta*. **2006**, 441, 35.
69. Grenci G.; Zanchetta E.; Pozzato A.; Giustina G. D.; Brusatin G.; Tormen M. High resolution spin-on electron beam lithography resist with exceptional dry etching resistance. *Applied Materials Today*. **2015**, 1, 13.
70. Zanchetta E.; Giustina G. D.; Grenci G.; Pozzato A.; Tormen M.; Brusatin G. Novel Hybrid Organic–Inorganic Spin-on Resist for Electron- or Photon-Based Nanolithography with Outstanding Resistance to Dry Etching. *Adv. Mater*. **2013**, 25, 6261.
71. Webb D.J.; Hatzakis M. Metal methacrylates as sensitizers for poly methyl methacrylate electron resists. *J. Vac. Sci. Technol.* **1979**, 16, 2008.
72. Abbas A.S.; Alqarni S.; Shokouhi B.B.; Yavuz M.; Cui B. Water soluble and metal-containing electron beam resist poly(sodium 4-styrenesulfonate). *Mater. Res. Express*. **2014**, 1, 045102.
73. Con C.; Dey R.; Ferguson M.; Zhang J.; Mansour R.; Yavuz M.; Cui B. High molecular weight polystyrene as very sensitive electron beam resist. *Microelectron. Eng.* **2012**, 98, 254.
74. Kim S.; Marelli B.; Brenckle M.A.; Mitropoulos A.N.; Gil E.-S.; Tsioris K.; Tao H.; Kaplan D.L.; Omenetto F.G. All-water-based electron-beam lithography using silk as a resist. *Nat. Nanotechnol.* **2014**, 9, 306.
75. Omenetto F.G.; Kaplan D.L. New opportunities for an ancient material. *Science*. **2010**, 329, 528.
76. Kim S.; Mitropoulos A.N.; Spitzberg J.D.; Tao H.; Kaplan D.L.; Omenetto F.G. Silk inverse opal. *Nature Photon.* **2012**, 6, 818.
77. Bhumiratana S.; Grayson W.L.; Castanedaa A.; Rockwood D.N.; Gil E.S.; Kaplan D.L.; Vunjak-Novakovic G. Nucleation and growth of mineralized bone matrix on silk-hydroxyapatite composite scaffolds. *Biomaterials*. **2011**, 32, 2812.
78. Chen W.; Ahmed H. Fabrication of 5–7 nm wide etched lines in silicon using 100 keV electron-beam lithography and polymethylmethacrylate resist. *Appl. Phys. Lett.* **1993**, 62, 1499.
79. Park J.; Lee S.-G.; Marelli B.; Lee M.; Kim T.; Oh H.-K.; Jeon H.; Omenetto F. G.; Kim S. Eco-friendly photolithography using water-developable pure silk fibroin. *RSC Adv.* **2016**, 6, 39330.
80. von Freymann G.; Lidermann A.; Thiel M.; Staude I.; Essig S.; Busch K.; Wegener M. "Three-Dimensional Nanostructures for Photonics. *Adv. Funct. Mater.* **2010**, 20, 1038.
81. Buitrago E.; Badia M.F.-B.; Georgiev Y.M.; Yu R.; Lotty O.; Holmes J.D.; Nightingale A.M.; Gueria H.M.; Ionescu A.M. Electrical characterization of high performance, liquid gated vertically stacked SiNW-based 3D FET biosensors. *Sensors Actuat. B Chem.* **2014**, 199, 291.
82. Soukoulis C.M.; Wegener M. Past achievements and future challenges in the development of three-dimensional photonic metamaterials. *Nat. Photonics*. 2011, 5, 523.
83. Vila-Comamala J.; Gorelick S.; Guzenko V.A.; David C. 3D Nanostructuring of hydrogen silsesquioxane resist by 100 keV electron beam lithography. *J. Vac. Sci. Technol. B.* **2011**, 29, 06F301.
84. Varghese L.T.; Fan L.; Wang J.; Xuan Y.; Qi M. Rapid and Low-Cost Prototyping of 3D Nanostructures with Multi-Layer Hydrogen Silsesquioxane Scaffolds. *Small*. **2013**, 9, 4237.
85. Tanenbaum D.M.; Olkhovets A.; Sekaric L. Dual exposure glass layer suspended structures: A simplified fabrication process for suspended nanostructures on planar substrates. *J. Vac. Sci. Technol. B.* **2001**, 19, 2829.
86. Osipowicz T.; van Kan J.A.; Sum T.C; J.L. Sanchez; Watt F. The use of proton microbeams for the production of microcomponents. *Nucl. Instr. Meth. Phys. Res.* **2000**, 161-163, 83.
87. Watt F.; Bettiol A.A.; van Kan J.A.; Teo E.J.; Breese M.B.H. Ion beam lithography and nanofabrication: a review. *Int. J. Nanosci*. **2005**, 04, 269.
88. Wanzenboeck H.D.; Waid S. Focused Ion Beam in B. Cui Eds., Recent Advances in Nanofabrication Techniques and Applications. **2011**, Chapter 2, pp 28-50.

89. Li W.-D.; Wu W.; Williams R.S. Combined helium ion beam and nanoimprint lithography attains 4 nm half-pitch dense patterns. *J. Vac. Sci. Technol. B.* **2012**, 30, 06F304.
90. Shi X.; Prewett P.; Huq E.; Bagnall D.M.; Robinson A.P.G.; Boden S. A. Helium ion beam lithography on fullerene molecular resists for sub-10 nm patterning. *Microelectron. Eng.* **2016**, 155, 74.
91. Pease R.F.W.; Han L.; Winograd G.; Meisburger W.D. Prospects for charged particle lithography as a manufacturing technology. *Microelectron. Eng*. **2000**, 53, 55.
92. Chang T.H.P.; Mankos M.; Lee K.Y.; Muray L.P. Multiple electron-beam lithography. *Microelectron. Eng.* **2001**, 57, 117.
93. Chang T.H.P.; Thomson M. G. R.; Kratschmer E.; Kim H. S.; Yu M.L.; Lee K.Y.; Rishton S.A.; Hussey B.W.; Zolgharnain S. Electron-beam microcolumns for lithography and related applications. *J. Vac. Sci. Technol., B.* **1996**, 14, 3774.
94. Klans J.M.; van Rooy T.L.; A Miniature Low Voltage SEM with High Resolution, Microscopy and Microanalysis 5 (Suppl. 2 Proceedings), *Microscopy Society of America,* **1999**, 322.
95. Shaw S.; Miller K.J.; Colaux J.L.; C. Ludovico. Optics-free, plasma-based lithography in inorganic resists made up of nanoparticles. *J. Micro/Nanolith. MEMS MOEMS.* 2016, 15, 031607.
96. Angelopoulos M.; Patel N.; Shaw J.M.; Labianca N.C.; Rishton S.A. Water soluble conducting polyanilines: Applications in lithography. *J. Vac. Sci. Technol. B.* **1993**, 11, 2794.
97. Morikawa J.; Ryu M.; Maximova K.; Balčytis A.; Seniutinas G.; Fand L.; Mizeikise V.; Lid J.; Wang X.; Zamengo M.; Wang X.; Juodkazis S. Silk fibroin as a water-soluble bio-resist and its thermal properties. *RSC Adv.* **2016**, 6, 11863.
98. Gatzert C.; Blakers A.W.; Deenapanray P.N.K.; Macdonald D.; Auret F.D. Investigation of reactive ion etching of dielectrics and Si in CHF_3/O_2 or CHF_3/Ar for photovoltaic applications., *J. Vac. Sci. Technol. A.* **2006**, 24, 1857.
99. Zhang C.; Yang C.; Ding D. Deep reactive ion etching of commercial PMMA in O2/CHF3, and O2/Ar-based discharges. *J. Micromech. Microeng.* **2004**, 14, 663.

Table of Contents (TOC)

